The United Nations University

GEOTHERMAL TRAINING PROGRAMME
Orkustofnun, Grensásvegur 9,
IS-108 Reykjavík, Iceland

Reports 1995
Number 2

THE ÖLKELDUHÁLS GEOTHERMAL FIELD, A COMBINED ANALYSIS OF RESISTIVITY TEM SOUNDINGS AND DOWN-HOLE DATA

Tafif Azimudin
PERTAMINA - Direktorat Eksplorasi dan Produksi,
Divisi Panasbumi,
Jl. Kramat Raya 59, Jakarta,
INDONESIA

ABSTRACT

The Ölkelduháls high-temperature geothermal field is situated within the Hengill volcanic complex. Interpretation of TEM soundings indicates that it is associated with a highly resistive body (>50 Ωm) below a conductive layer (<5 Ωm) covering an area of about 20 km^2. The resistivity distribution is generally divided into three layers, an upper layer of high resistivity (>50 Ωm), a middle layer of very low resistivity (<10 Ωm) and a lower layer of high resistivity (>20 Ωm). The results of the TEM soundings were compared with those of Schlumberger soundings giving similar results, but demonstrating the better resolution and accuracy of the TEM data. In the winter 1994-1995, well ÖJ-1 was drilled as the first exploration well in the area. Several downhole geophysical measurements were conducted during and after drilling. Both TEM soundings and resistivity logs identified the top of the geothermal reservoir at 120 m. Porosity values obtained from geophysical log calculation and core analysis show good correlation. Analyses of well tests indicate three major feedzones at 820-827, 948-963 and 1000-1035 m. The permeability of this well is very high, especially of the bottom feedzone, with an estimated productivity index of about 0.8×10^{-11} m^3/s bar.

1. INTRODUCTION

1.1 Scope of study

The Hengill volcanic complex is located in the volcanic rift zone in SW-Iceland about 30 km east of the capital Reykjavík. The high-temperature geothermal area associated with it, is among the largest in Iceland, covering about 100 km^2. It is divided into at least five geothermal fields, one of which is the Ölkelduháls field located in the central part. The other fields are Nesjavellir, where a recent power plant is operated by the Reykjavík District Heating, Hengladalir, West-Hengill and Hveragerdi.

Fumaroles and hot springs in the Hengill area are distributed on a zone from Nesjavellir in the north across the Hengill mountain through Ölkelduháls to Hveragerdi in the south (Figure 1). Exploration of the Hengill area has extended over several decades with special attention to the Nesjavellir area in the

the Hengill area has extended over several decades with special attention to the Nesjavellir area in the eighties (Björnsson et al., 1986; Gunnarsson et al., 1992). It was not until 1992 that the interest focussed on the Ölkelduháls field, when a central loop transient electromagnetic (TEM) survey was carried out. Encouraging results of the geoscientific survey led to the drilling of the first exploratory well ÖJ-1 in the winter 1994-1995. Several downhole measurements consisting of temperature, pressure and lithological logs were conducted during and after drilling. Furthermore, a core sample was taken at 794.7-798.1 m depth.

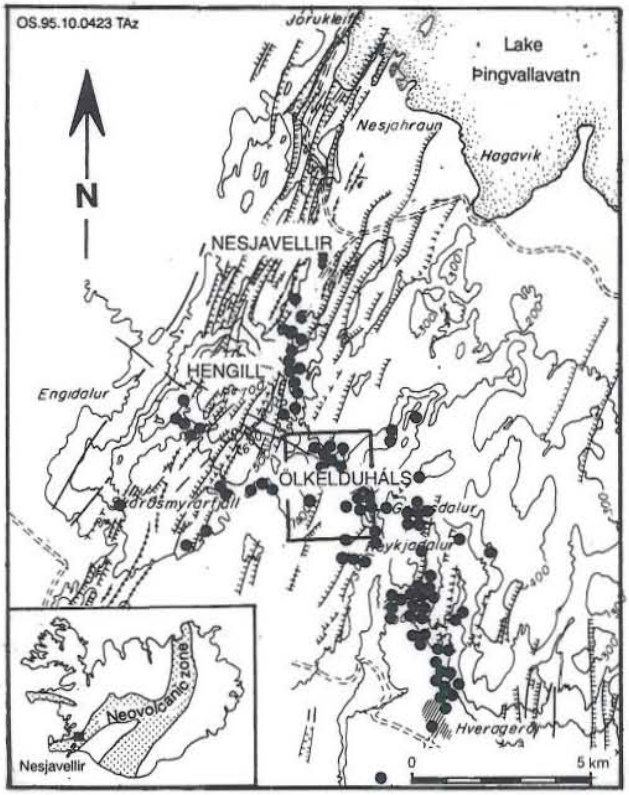

FIGURE 1: Tectonic map of the Hengill area. The location of active geothermal manifestation (fumaroles and hot springs) is shown with black dots. The Ölkelduháls field is situated within the square (after Gunnarsson et al., 1992).

The main objects of this report are to analyse and interpret both TEM resistivity data in the vicinity of well ÖJ-1 and downhole logs in order to correlate surface and subsurface resistivity. Furthermore, to obtain subsurface information on the physical characteristics of the geothermal system according to downhole logging data.

This project report is the final part of a six months training course for the Fellows of the United Nations University, Geothermal Training Programme at Orkustofnun, the National Energy Authority of Iceland.

1.2 Tectonics and geological setting

A zone of active volcanism and tectonism crosses Iceland from southwest to northeast. It is divided into two parallel branches in the south (see inlet on Figure 1), where the axial rift zone is under tensional stress parallel to the spreading direction. Rocks in the axial rift zone are interglacial lava flows and subglacial hyaloclastites, and are younger than 0.7 million years (Björnsson et al., 1986). The Hengill area is located in SW-Iceland within the western branch of the active volcanic zone (Saemundsson, 1979).

Three major volcanic systems are situated within the Hengill area, the presently active Hengill and Hrómundartindur, and the extinct Hveragerdi volcanic system. Each volcanic system is intersected by a fissure swarm which has the structure of a nested graben. The geological formations in the Ölkelduháls area consist primarily of basaltic hyaloclastites and lavas related to the Upper Pleistocene and Postglacial series. The majority of faults, fissures and hyaloclastite ridges strike NE-SW and are shown in Figures 1 and 2 (Saemundsson et al., 1990). Fumaroles and hot springs are distributed along the faults and fissures. An altered rock zone is formed due to the interaction between geothermal fluids and rocks surrounding the surface geothermal manifestation.

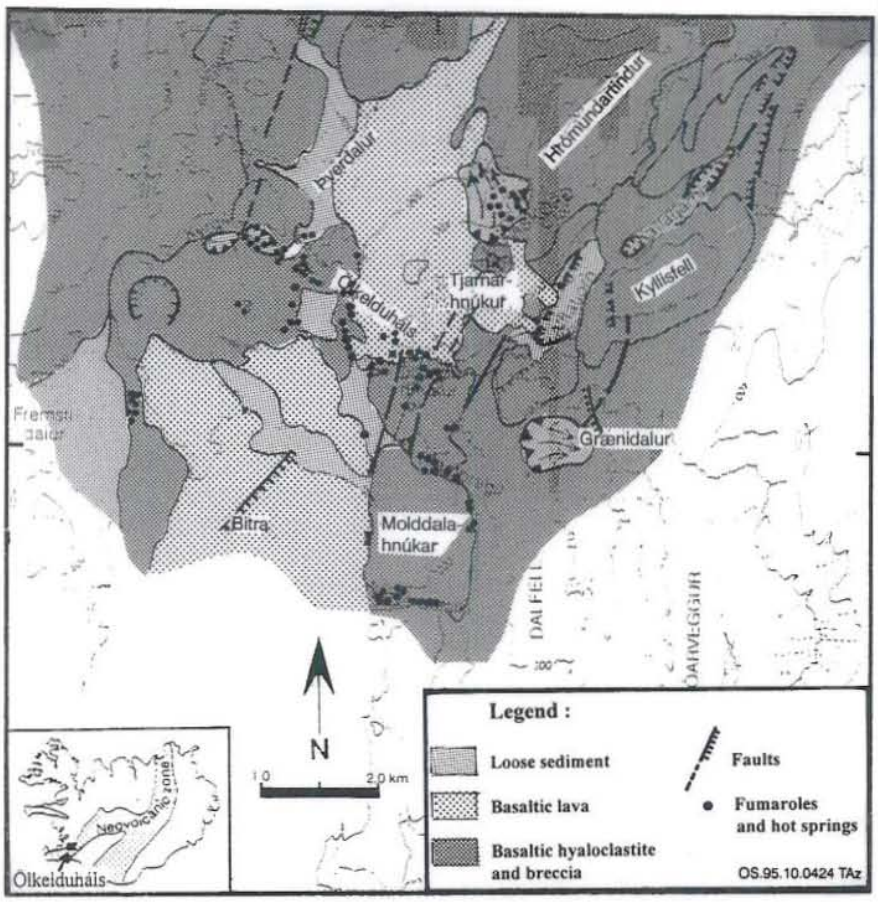

FIGURE 2: Simplified geological map of the Ölkelduháls field (mod. from Saemundsson et al., 1990)

2. THE CENTRAL-LOOP TEM SOUNDING SURVEY

The high-temperature geothermal areas in Iceland are located in the volcanic zones and are largely covered by fresh basaltic lavas. Hence, electric current injection into the ground can be difficult, making the use of direct current electrical methods, like Schlumberger sounding difficult. This is one of the main reasons that the central-loop transient electromagnetic method (TEM) has replaced the conventional Schlumberger sounding in geothermal exploration in Iceland. TEM is faster and easier in data collection, requiring less manpower. It is less sensitive to local resistivity variations and gives better downward focussing in 1-D interpretation where more time consuming 2-D or 3-D interpretation is necessary for DC-methods, and stronger signals in areas of interest for geothermal prospecting.

2.1 Basic principles

In the central-loop TEM sounding method, electric currents are induced in the ground by a time varying magnetic field. A loop of wire is placed on the ground and a constant magnetic field of known strength is built up by transmitting a constant current in the loop and then the current is abruptly turned off. The decaying magnetic field induces electric currents in the ground (Figure 3). The current distribution in the ground induces secondary magnetic field, also decaying with time. The decay rate of the secondary magnetic field is monitored by measuring the voltage induced in a receiver coil at the centre of the

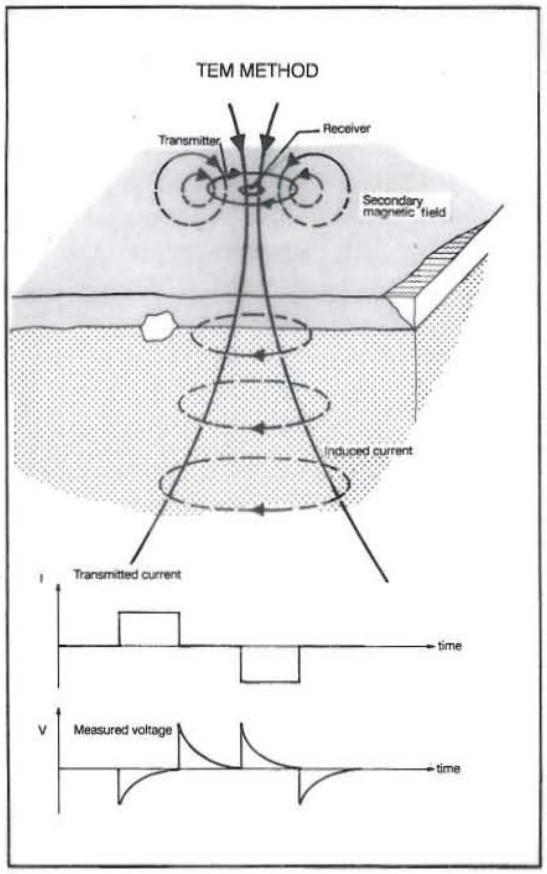

FIGURE 3: The central-loop TEM sounding configuration (Hersir and Björnsson, 1991)

transmitter loop. The current distribution and the rate of decay of the secondary magnetic field depend on the resistivity structure of the earth. The rate of decay, recorded with time after the current in the transmitter loop is turned off, reflects the subsurface resistivity structure. The depth of penetration in the central-loop TEM sounding depends on the geoelectrical section and how long the induction in the receiver can be traced in time before it is drowned in background noise.

The TEM signal is usually presented as an apparent resistivity given by the following formula (Hersir and Björnsson, 1991; Árnason, 1989):

$$\rho_a(r,t) = \frac{\mu_o}{4\pi}\left[\frac{2\mu_o A_r n_r A_s n_s}{5\, t^{5/2} V(r,t)}\right]^{2/3} \qquad (1)$$

where

t = time elapsed, after the current in the transmitter loop is turned off (μs)
A_r = cross-sectional area of the receiver loop (m^2)
n_r = number of windings in the receiver loop
$V(r, t)$ = transient voltage (V)
μ_0 = magn. permeability in vacuum (henry/m)
A_s = cross-sec. area of the transmitter loop (m^2)
n_s = number of windings in the transmit. loop

2.2 Data acquisition and analysis

The central-loop TEM sounding field equipment used in the Ölkelduháls area consists of a generator, transmitter, receiver and receiver/transmitter loops. There are two receiver loops, a small coil with an effective area of 100 m^2 and a flexible coil with an effective area of 8,000 m^2. A square transmitter loop of 300 m side length was used. The transmitter and receiver are synchronized through crystal clocks and the data are digitally recorded as voltage versus time in the receiver. The current turn-off time was also recorded. This is the time it takes to turn the current off from its maximum value to zero, and depends on the size of the transmitter loop. The data were recorded over high and low frequency sweeps. Preliminary data analysis includes stacking of the recorded voltages. The stacked data are then edited to remove any spurious measurements due to electromagnetic noise and the result is then averaged to obtain induced voltage as a function of time. The induced voltage is then used to calculate apparent resistivity as a function of time.

A nonlinear least-square inversion programme TINV for TEM soundings has been used for 1-D interpretation (Árnason, 1989). The aim is to determine the resistivity layered model whose response reproduces the measured values as closely as possible. TINV was developed for an IBM PC and is written in standard FORTRAN 77 and can, in principle, be implemented on any machine supporting that language.

2.3 The TEM survey in Ölkelduháls

Measurements of 35 TEM soundings in the Ölkelduháls area were carried out during the period of 1991-1992 by Orkustofnun and Hitaveita Reykjavíkur (Árnason, 1993). The data from 12 stations surrounding well ÖJ-1 were processed by the author (Figure 4 and Appendix I).

Ten of these soundings are on a line trending NE-SW (Figure 5). The resistivity distribution can, in general, be divided into three layers. The uppermost layer generally has a high-resistivity (>50 Ωm), except at station 8 where the resistivity is low (5.9 Ωm), due to surface geothermal activity. The second layer has a very low resistivity, generally less than 10 Ωm and in the central part of the cross-section some times less than 5 Ωm. Below the low-resistivity layer is a high-resistivity body with resistivity higher than 20 Ωm, like a core inside a low-resistivity coat (Figure 5).

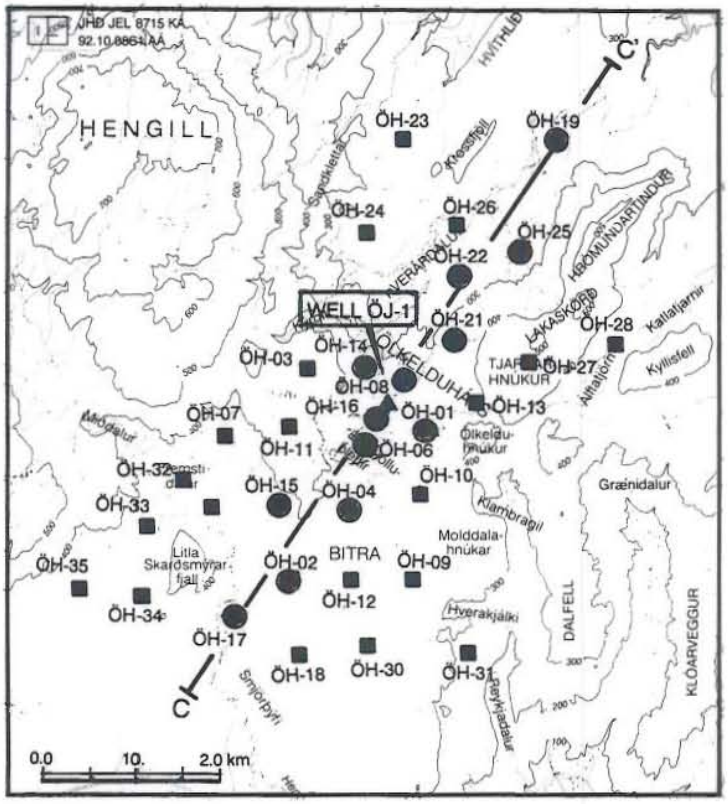

FIGURE 4: Location map of the TEM sounding stations in the Ölkelduháls field (black squares and dots); the stations processed by the author are shown with dots; also shown is the resistivity cross-section line C-C' (mod. from Árnason, 1993)

The presence of a high-resistivity body below a conductive layer is typical for high-temperature fields in Iceland. The relationship between resistivity and other physical parameters in basaltic geothermal systems in Iceland has been studied (Árnason and Flóvenz, 1992 and Georgsson et al., 1993). They can be summarized as follows (Figure 6)

1. In young basaltic rocks with no alteration, the resistivity is controlled by the number and the mobility of ions in water, as described by Archie´s law and general temperature relationships;

2. Minor alteration of the basalts leads to the formation of thin and highly conductive layers of clay minerals, such as smectite at the interfaces of water and rock in the pores. In freshwater geothermal systems, interface conduction takes over from ionic conduction as the dominant conduction mechanism. In brine geothermal systems ionic conduction continuos to dominate;

3. At elevated temperatures secondary minerals start to deposit in the pores, reducing porosity with depth. When high-temperature minerals such as epidote and chlorite with less cation exchange capability replace the clay minerals, the resistivity increases abruptly. This is due to a sudden change of conduction mechanism, from interface conduction to ionic conduction, which occurs at temperatures around 250°C. This phenomenon is not observed in brine systems, where ionic conduction generally dominates.

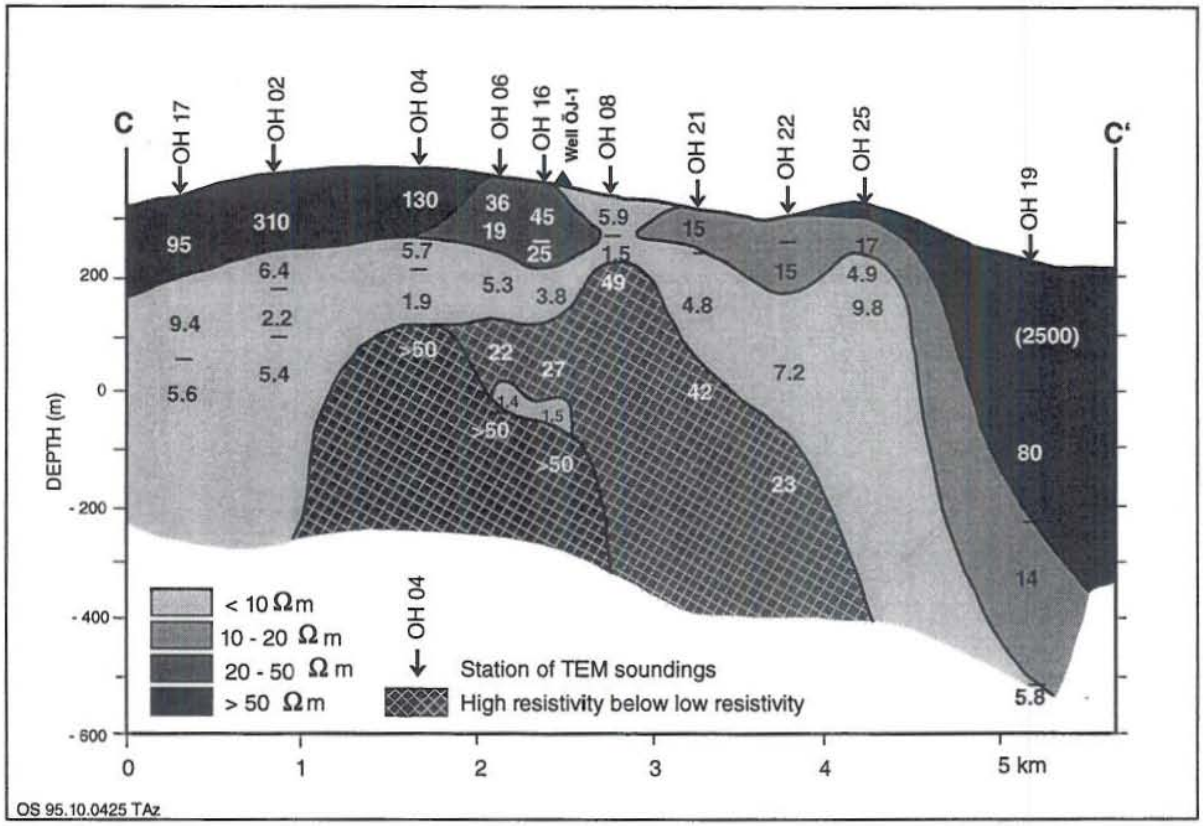

FIGURE 5: Resistivity cross-section C-C'

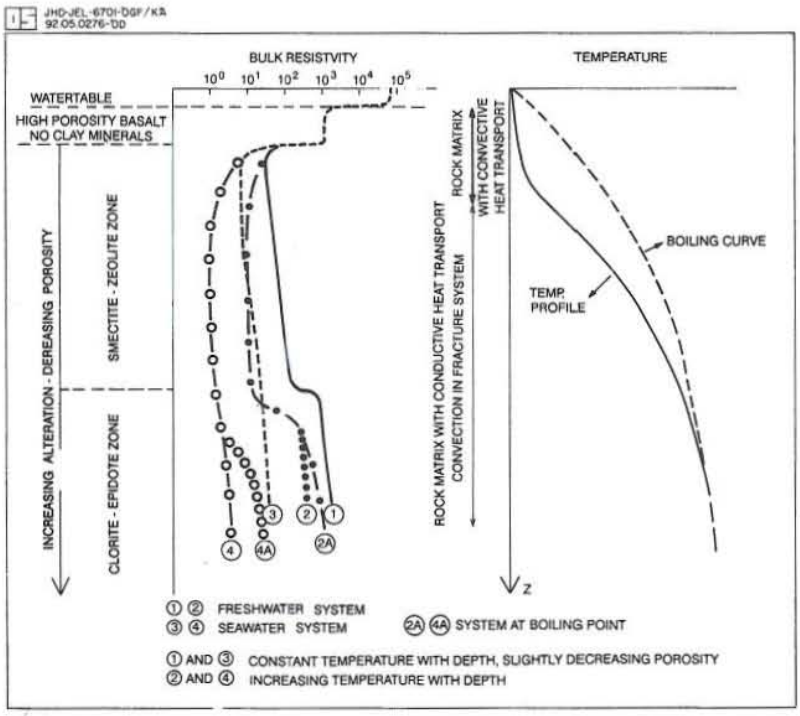

FIGURE 6: A schematic picture of the relationship between bulk resistivity, porosity, temperature and alteration stage of basaltic rock (after Árnason and Flóvenz, 1992)

Analysis of the alteration of drill cuttings from well ÖJ-1 (Franzson, pers. comm.) shows that this relationship applies to the Ölkelduháls data, with wairakite and epidote appearing around 300 m depth. The formation temperature on the other hand is only about 198°C. This can be explained by the alteration which shows evidence of recent changes in the thermal regime of the well, with calcite overprinting the older high-temperature minerals. This shows that the system has recently experienced some cooling.

Figures 7 and 8 show the resistivity at 250 and 100 m a.s.l. respectively (adapted from Árnason, 1993). The results of the TEM sounding

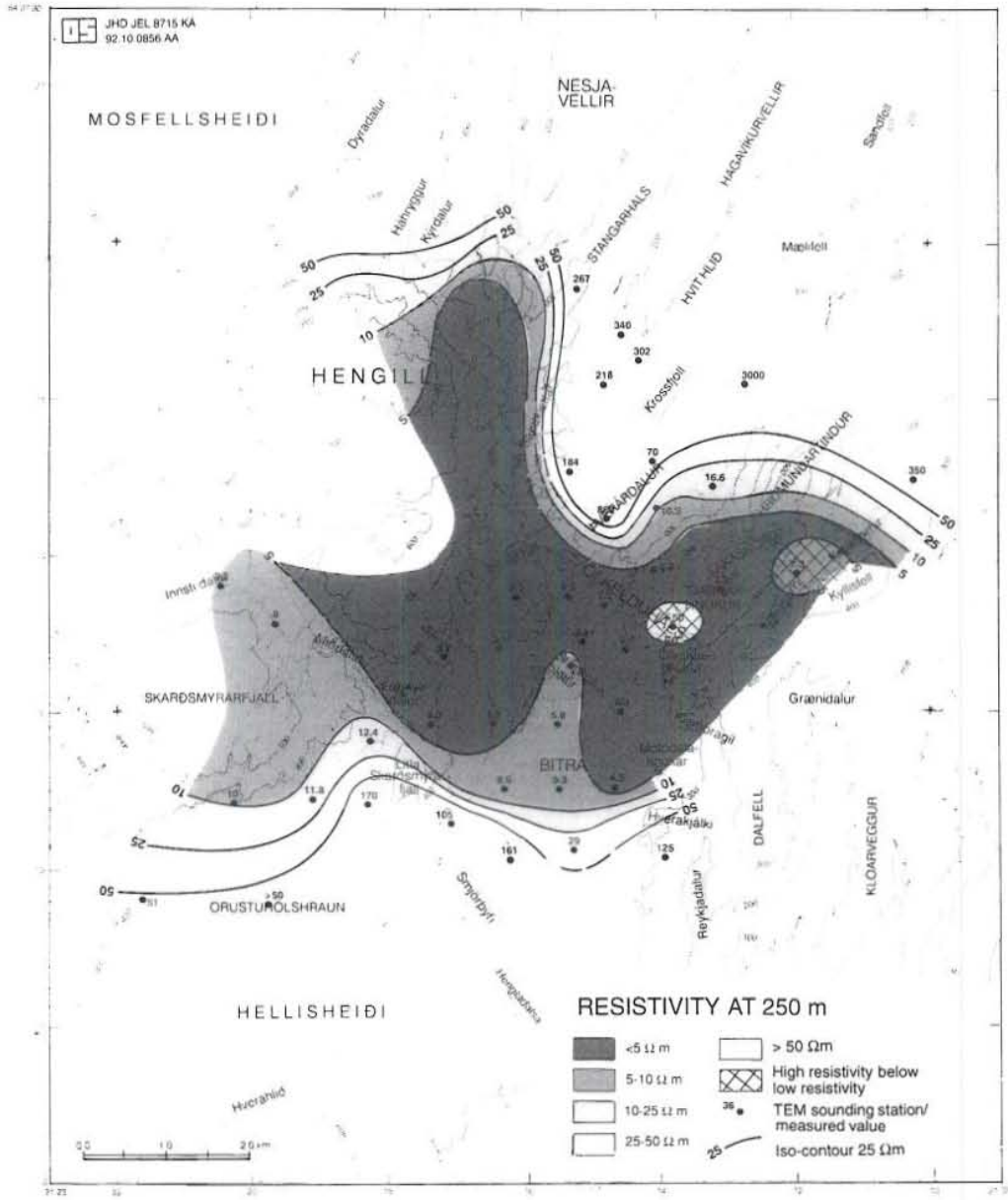

FIGURE 7: Resistivity map of the Ölkelduháls area at 250 m a.s.l. (after Árnason 1993)

survey can be summarized as follows: The Ölkelduháls high-temperature geothermal field is associated with a highly conductive layer at 250 m a.s.l. covering an area of about 20 km^2, with a resistivity less than 5 Ωm. The lineation of the low-resistivity contour is elongated in east-west direction across the main fissure direction, indicating a high-resistivity boundary between Ölkelduháls and Nesjavellir fields in the northern part and Hveragerdi in the southern part. The depth to the top of the low-resistivity layer varies from several tens of metres to a few hundred metres near the boundaries of the geothermal area. A striking feature is the presence of a high-resistivity body, below the low-resistivity layer, at the centre of the field. This becomes more clear at 100 m a.s.l. where a high-resistivity layer (>20 Ωm) more or less, replaces the low-resistivity layer.

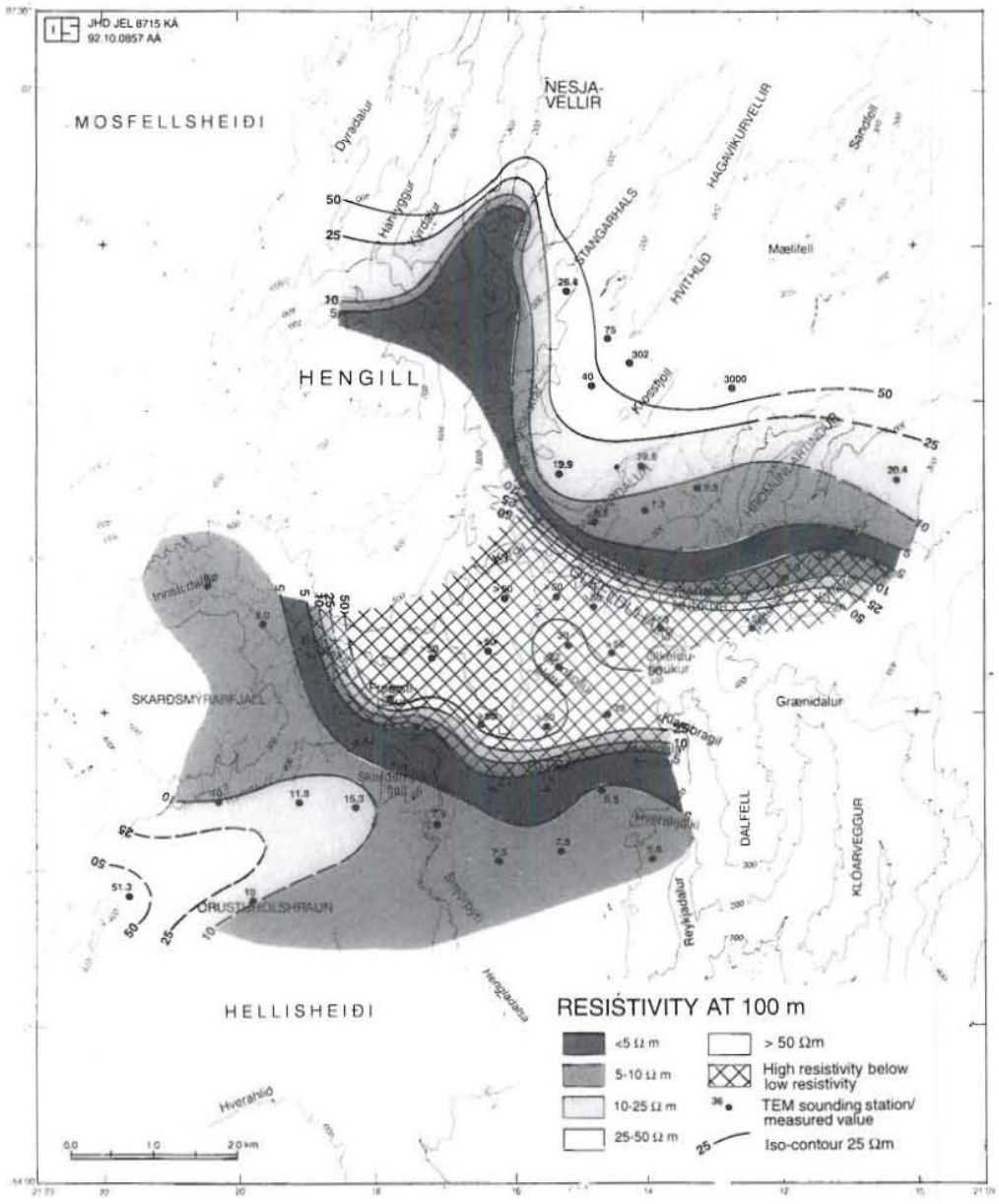

FIGURE 8: Resistivity map of the Ölkelduháls area at 100 m a.s.l. (after Árnason, 1993)

2.4 Comparison of TEM and Schlumberger soundings

For comparison, TEM and Schlumberger soundings were collected at exactly the same location in the Geitafell area about 20 km southwest of the Ölkelduháls field. Figure 9 shows the curves and 1-D interpretation of the TEM soundings (GEITA300) and the Schlumberger soundings (REF1 and REF2), where REF1 and REF2 were conducted with the directional arrays of the Schlumberger arrangement at about the right angle to each other. The best inversion results were selected in order to test the resolution of both methods.

The first layer corresponds to basaltic lavas above groundwater level. The resistivity is very high, about 25,000 Ωm, and well defined in the Schlumberger soundings, but not in the TEM sounding as it is too shallow. Therefore, the starting value for the TEM model was adopted from the Schlumberger

soundings. The thickness, however, is well defined in both, but probably best in the TEM soundings, 75 m. The second layer represents fresh basaltic lavas below groundwater level. It is well defined in the TEM and one of the Schlumberger soundings (REF1) with a resistivity of about 2,000 Ωm and a thickness of 140 m. In REF2 the resistivity is higher and the layer appears thinner. Below this, the resistivity decreases with increasing alteration of the rocks. It is apparent that the best accuracy and resolution are obtained from the TEM soundings. They show a layer of 500 Ωm and 260 m, and then another of about 100 Ωm and 210 m thickness and finally a layer of low resistivity of about 20 Ωm. This is in good agreement with the resistivity data in the surrounding area. The Schlumberger soundings instead show a 500-600 m thick 200-500 Ωm layer with a poorly defined low-resistivity layer below it.

Similar comparison was done for the Ölkelduháls area, where the TEM sounding OH01 was compared with a nearby Schlumberger sounding (Figure 10). It must however be stressed that the location is not exactly the same. The surface layers are very different. As expected, the resistivity is poorly defined in the TEM sounding, but the thicknesses are similar in both soundings.

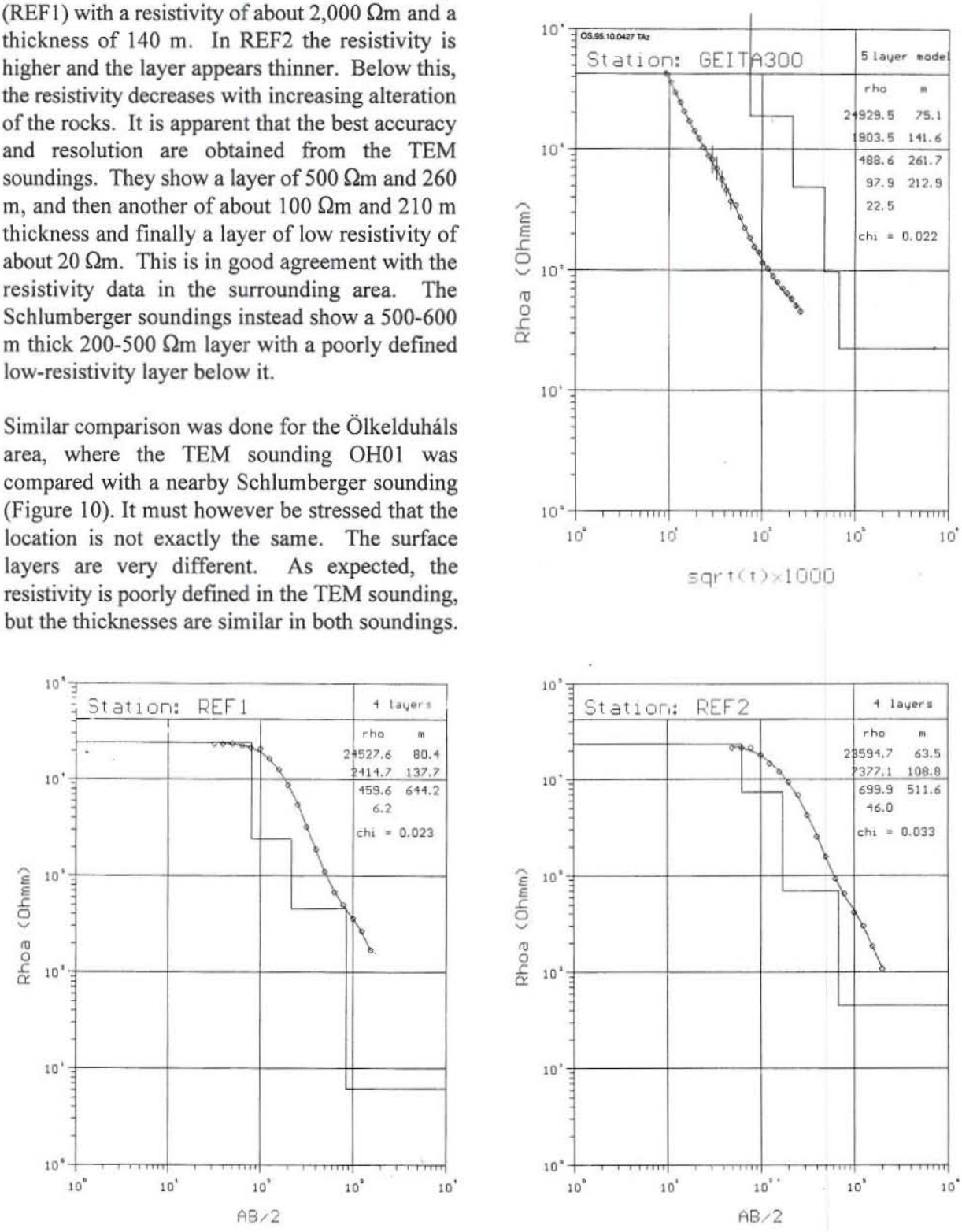

FIGURE 9: TEM (GEITA300) and Schlumberger (REF1 and REF2) sounding curves with interpretation, all measured at the same location at Geitafell in the S-Hengill area

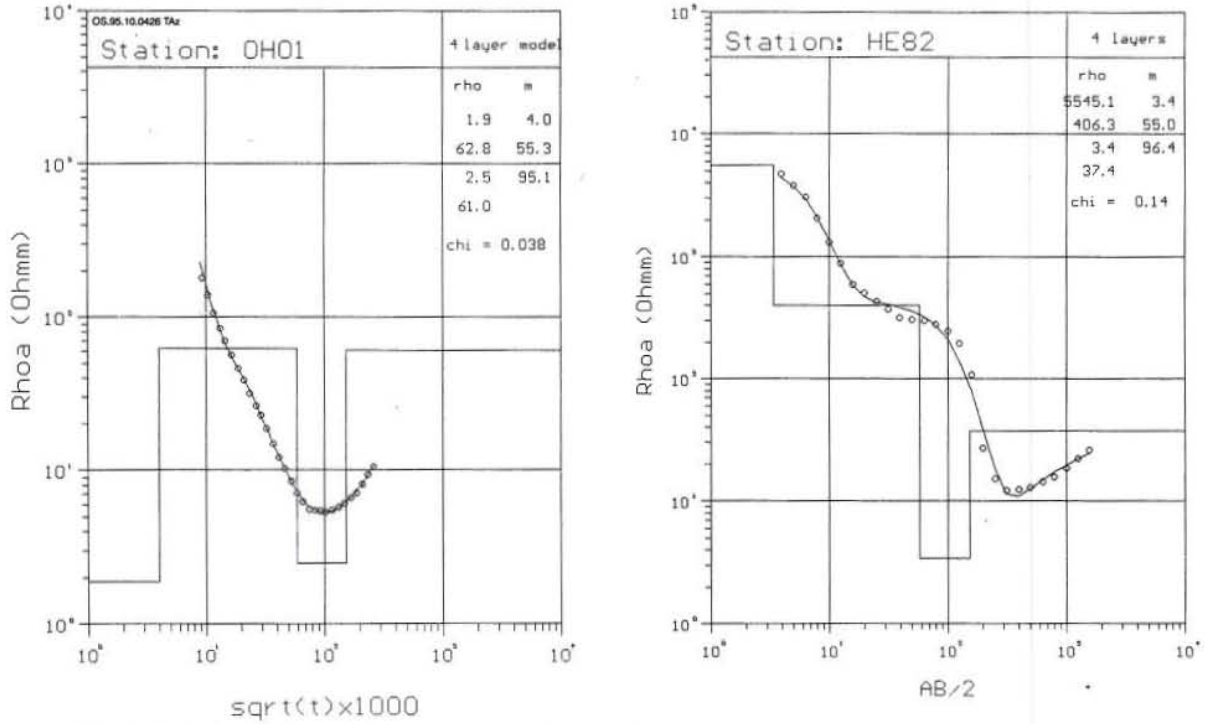

FIGURE 10: TEM sounding curve OH01 and Schlumberger sounding curve HE82 from the Ölkelduháls area with 1-D interpretation

Below, at a depth of about 59 m, both methods show a low-resistivity layer of about 3 Ωm (2.5/3.4 Ωm) and 95 m thickness. Further down both methods show increasing resistivity, 61 Ωm in the TEM sounding but 37 Ωm in the Schlumberger sounding.

Generally this comparison shows that there is good agreement between the two methods. The Schlumberger method defines better the resistivity of the surface layers, but the resolution of the TEM is better at deeper levels.

3. ANALYSIS OF DOWNHOLE DATA IN WELL ÖJ-1

3.1 Data sources

Well ÖJ-1 is the first exploration well drilled in the Ölkelduháls field. It was drilled during the period October 10, 1994 to January 22, 1995, the UTM coordinates are X=658,674.65; Y=399,188.00 and Z=360.77 m. Well ÖJ-1 was drilled to a total depth of 1035 m. The well was designed as follows, a 18 5/8" conductor casing from surface to 70.7 m with 21 1/4" flange pipe, a 13 3/8" anchor casing to 293.6 m, a 9 5/8" production casing to 770.4 m and a 7" slotted liner from 726.2 to 1006 m. The drilling history and the well design have already been presented in three preliminary reports by Gudmundsson, et al. (1994, 1995a, and 1995b). The design of well ÖJ-1 is shown in Figure 11 together with caliper logs.

In order to provide sufficient circulation water for drilling of ÖJ-1, two shallow wells were drilled before the drilling of well ÖJ-1 started. Observations of circulation losses plus downhole temperature and pressure data in ÖJ-1well showed that three aquifer systems were intersected by the well, a cold groundwater system (8°C) at 14 m, warm groundwater (34.4°C) at 68 and 120 m and geothermal aquifers from 400 m to the bottom of the well.

The downhole logging data collected in ÖJ-1 during and after drilling consist of lithological logs, temperature logs and pressure logs. The total number of downhole logs to date is 112, giving a cumulative depth of 79 km. Of these, 42 are temperature logs, 11 are pressure logs and 26 km are lithological logs. Lithological logging was conducted at three different depth intervals, i.e. before running the 13 3/8" anchor casing, the 9 5/8" production casing and 7" slotted liner. The most recent temperature and pressure logs were conducted at flowing condition. An injection test was conducted during the completion test, where an 11°C cold water was injected in steps while measuring the downhole temperature and pressure.

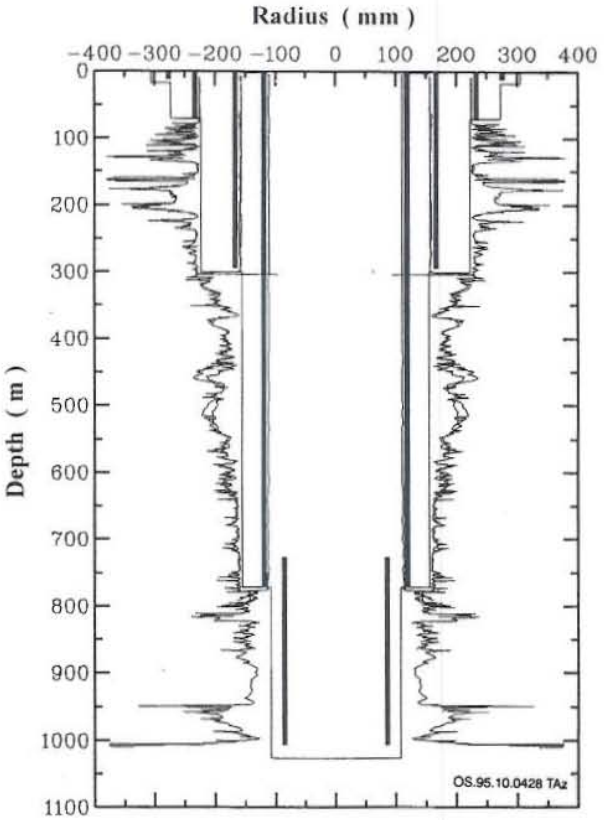

FIGURE 11: A schematic figure of the downhole profile of well ÖJ-1 and results of caliper logs

3.2 Evaluation of formation temperature and pressure

Well ÖJ-1 was allowed to warm up for eight months before discharging. The formation temperatures and pressures in the lower half of the well are therefore determined by temperature and pressure profiles collected during the warming up period.

Figure 12 shows the measured temperature and pressure profiles and the estimated formation temperatures and pressures. In this case, the formation temperature profile can be divided into two parts. The uppermost part, which ranges from surface down to 120 m depth and is controlled by cold and warm aquifer systems, which water levels are at 14 and 33 m respectively. From 120 m down to approximately 400 m we have a conductive caprock layer where the temperature rises from 20 to 200°C. Formation

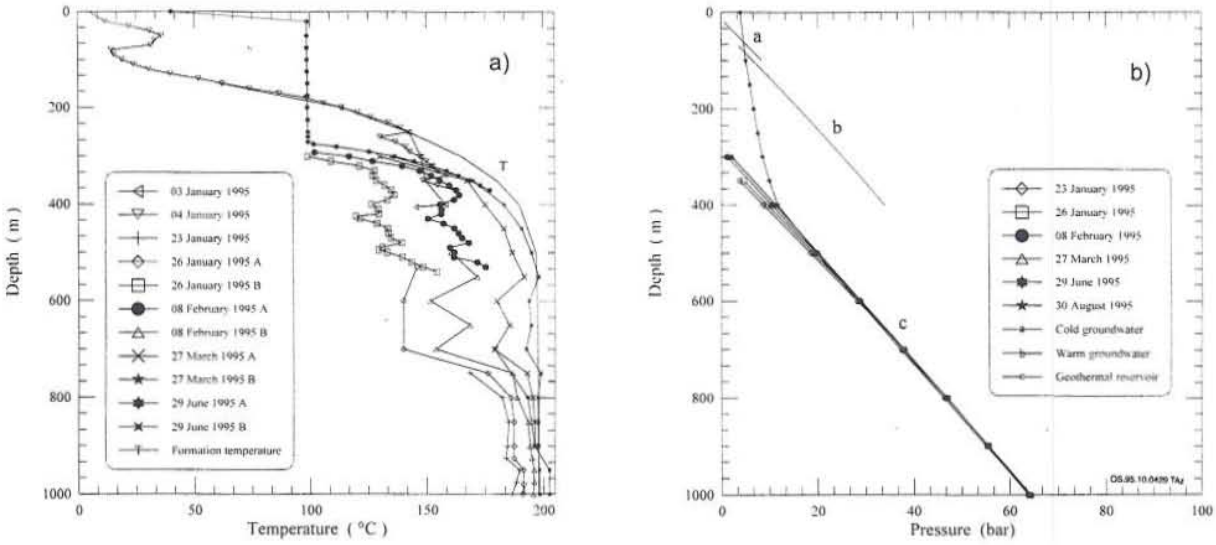

FIGURE 12: Temperature (a) and pressure (b) profiles collected in well ÖJ-1 during and after drilling along with estimated formation temperature and initial pressure

temperature down to 400 m is based on temperature profiles that were measured on January 4, 1995 after weeks of warming up. Finally we have the geothermal reservoir from 400 m depth to the bottom of the well. Formation temperature in this depth is based on a temperature log collected on August 30, 1995, after 8 months of warming up. It shows isothermal conditions in the reservoir indicating a convection system of high vertical permeability.

The initial pressure profile is divided into three parts. The two first are based on water level observations during drilling, when well ÖJ-1 encountered feedzones at 14, 68 and 120 m depth. The shallow reservoir pressure was calculated according to the recorded water level and water density at the estimated formation temperature, using the programme PREDYP (Björnsson, 1993). For the deep reservoir the initial pressure is simply based on the last pressure log collected before discharge (August 30, 1995). There is a slight difference in pressure potential between the cold and the warm aquifer as observed in these water levels (14 and 33 m respectively). The pressure potential of the geothermal system is on the other hand, much lower than that of the shallow aquifers as is clearly demonstrated in Figure 12.

3.3 Lithology logs

Commonly, the lithological studies in well-site geology have mainly been done on cores or cuttings recovered during the drilling. In lithological logging, physical parameters related to the properties of the rocks penetrated by drilling are measured. In this chapter a description is given on some of the lithological logs and interpretation methods applied to well data from ÖJ-1 in the Ölkelduháls field.

Caliper log

The caliper log gives the diameter of the well. It is very important for well size correction in well log analysis. There are several types of measurement probes, the ordinary type is a three-arm caliper, but tools with one up to 60 arms are available. The arms are generally opened by an electrical motor inside the tool. Due to the electrical cable and downhole electronics, high-temperature wells must usually be quenched with cold water before the logging can be carried out. During logging, the probe is lowered to the bottom of the well, the arms are opened by the motor in the probe and the log is run continuously from the bottom of the well to the top. Diameter variations in the borehole are detected by changes in the deflection of the caliper arms, which are reflected in resistance changes inside the tool.

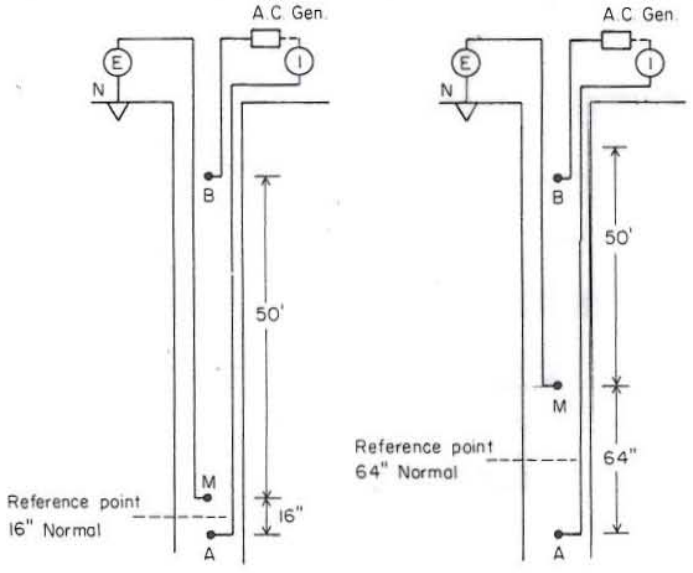

FIGURE 13: Electrode arrangements for the 16" and 64" normal resistivity log configurations (Keys and McCary, 1971; after Stefánsson and Steingrímsson, 1980)

Resistivity log

The resistivity log is performed in order to measure resistance along the formations in the borehole. The resistivity depends on the physical properties of the rocks, on the properties of the reservoir fluid and on the temperature. The current depends on the amount of ions present in the solution and on temperature. As the temperature of a solution increases, its viscosity decreases and the ions obtain higher mobility, which is equivalent to lower resistivity.

Figure 13 presents a sketch of the normal configuration of a resistivity tool. It is composed of four electrodes with two of them fixed on the logging

sonde. The third electrode is placed at the surface (mud pit), and armour of the logging wire line is used as the fourth electrode. During logging a constant current is passed through the formation via current electrodes *A* and *B*, and voltage is measured between potential electrodes *M* and *N*. The resistivity of an infinite homogeneous medium is given by the relation (Stefánsson and Steingrímsson, 1980)

$$\rho = 4\pi AM \frac{V}{I} \qquad (2)$$

Where *AM* is the distance between the two electrodes fixed on the logging sonde. The standard electrode spacing is generally 16" and 64".

In a non-uniform medium, the resistivity by the above relation is an apparent resistivity. The normal configuration resistivity will show the apparent resistivity variations of the medium surrounding the sonde, and will include the well itself. The determination of the true rock resistivity will therefore include elimination of wellbore effects (fluid resistivity and well size) and temperature as well as the effects of limited bed thickness of the adjacent lithological units.

Natural gamma ray log

The natural radioactivity of the rock formation is due to the presence of radioactive isotopes in the formation. Therefore, natural gamma ray logging is conducted in order to measure the electromagnetic radiation emitted from an atomic nucleus during radioactive decay. The isotopes that are mainly responsible for the radiation are potassium (^{40}K) and those involved in the decay series of uranium (^{238}U) and thorium (^{232}Th).

The two types of detectors generally used to measure the radioactivity, are the Geiger Müller counter which measures the total gamma ray intensity, and the scintillation counter that measures a certain energy spectrum of the gamma radiation. The count rate measured by a gamma ray tool at each depth in a borehole is related to the concentration of the radioisotopes in the formation, which is called the radioactivity of that formation.

Investigations in Iceland have shown that the gamma ray radioactive volcanic rock in Icelandic is related to the SiO_2 content in the rock. Geochemical evidence supports this correlation as the content of radioactive isotopes increases when going from basaltic to acidic igneous rocks (Stefánsson et al., 1982; Stefánsson and Steingrímsson, 1980). The natural gamma ray log is, therefore, used to identify the acidic rock, and as a guideline to correlate the rock formations between wells.

Neutron-neutron log

Neutrons are electrically neutral particles having a mass equal to the hydrogen atoms present in the formation, therefore, neutron-neutron logs are used in porosity investigations. When a neutron source is placed in a borehole, high energy neutrons are emitted from the source. They are slowed down through several collisions with the nuclei of the formations material until the thermal state is reached. In the thermal state the neutron will be captured by a nucleus and the capture will be accompanied by emission of gamma radiation. The slowing down of neutrons is therefore primarily controlled by the abundance of hydrogen (water) in the formation (Stefánsson and Steingrímsson, 1980).

The neutron logging tool consists of a neutron source and a detector, either a slow neutron detector (He^3) for the detection of thermal neutrons or gamma detector (GM-counter) which detects the gamma ray intensity emitted upon the capture of a neutron.

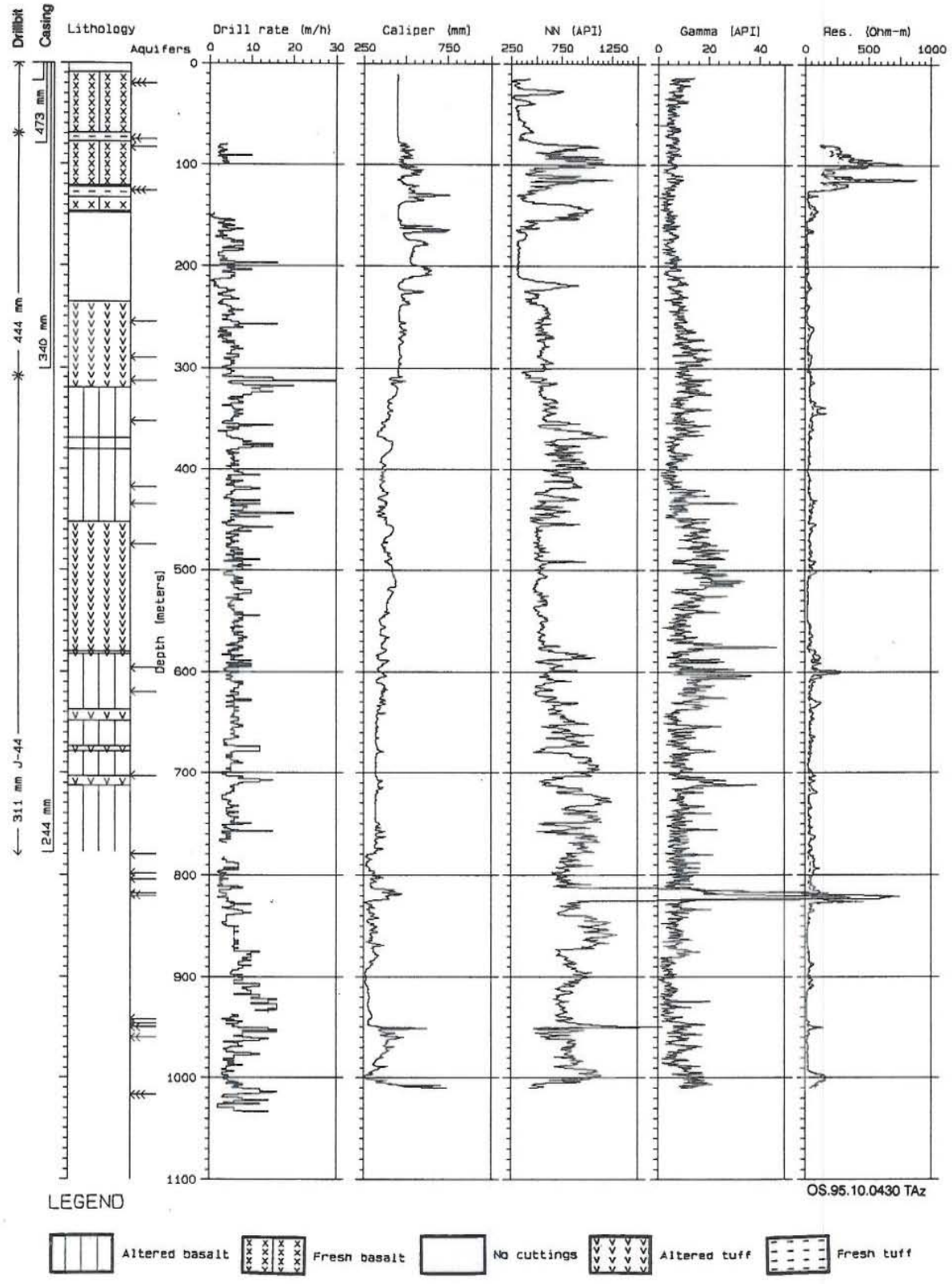

FIGURE 14: Lithology and raw data of lithological logs in well ÖJ-1

3.2.1 Estimating reservoir porosity and SiO_2 content

It is of interest to convert the lithological logs from well ÖJ-1 to reservoir properties such as porosity and silica content. The calculated properties can be compared with the physical properties of the core sample which was taken at 794.7-798.1 m depth in well ÖJ-1. Figure 14 shows the geological section based on

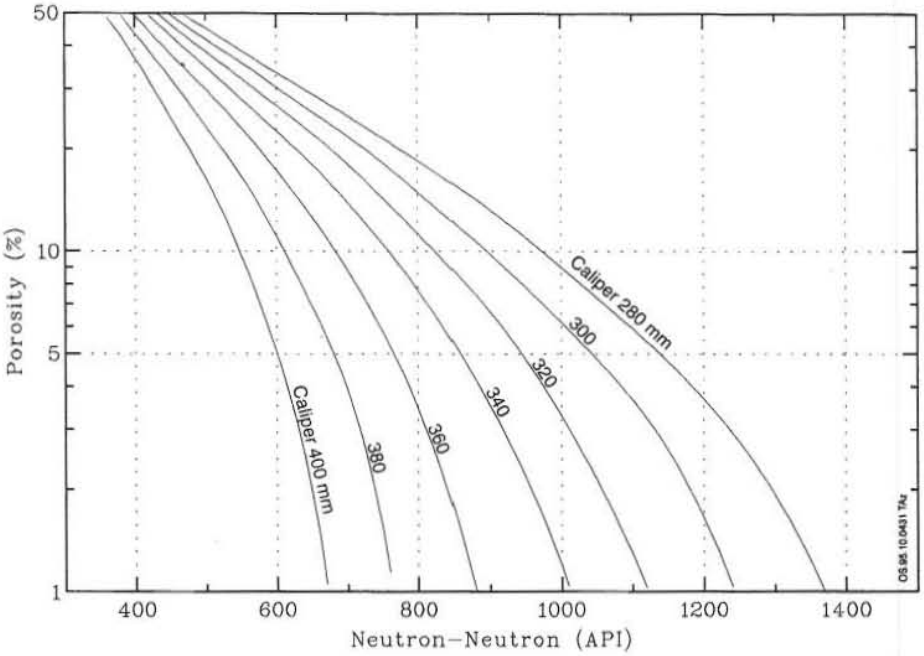

FIGURE 15: Neutron intensity and borehole diameter interpolation curves for porosity calculations

drill cuttings analysis, location of aquifers, drill penetration rate, the caliper, neutron-neutron, gamma and resistivity logs of the formation (solid line represents 16" registration). These data were collected continuously either during drilling or at the end of each of the three drilling phases (before installation of safety casing, production casing and liner).

Porosity

Formation porosity is estimated from the neutron-neutron log values using the diameter of the borehole as a correction factor. The BHMPOR programme (Arason, 1993), which is based on interpolation to calculate the porosity values from measured neutron intensity and diameter of the borehole (Figure 15), was used to determine the porosity at well ÖJ-1. However, the depth interval 0-235 m had to be omitted. The exceptionally large wellbore diameter (>460 mm) and rapid diameter changes over short intervals led to unrealistic porosity calculations and hence it is ignored.

The calculated porosity profile shown in Figure 16 ranges in porosity between 0-45%. The lithology of well ÖJ-1 can be divided into layers of basalt lavas and tuff. Figure 17 shows porosity histograms for these two types of rock. The figure shows that the tuff porosity is generally much higher than that of the basaltic lavas. The mean porosity for tuff is 14% whereas the mean porosity for basaltic lavas is 9%. The porosity difference is due to the mechanism of solidification, where the basalt is crystallised slowly allowing gas bubbles to escape from the molten lava. The tuff, on the other hand, is formed by explosive volcanism, where the lava solidifies with a lot of entrapped gas bubbles.

SiO_2 content

The gamma rays emitted by rocks are in general associated with the presence of radioactive elements like potassium (^{40}K), uranium (^{238}U) and thorium (^{232}Th). Experimental work has shown that the abundance of these elements is related to the silica content of the rock, according to the following equation, where, I_0 is the intensity of gamma radiation in API units and C is a correction factor due to the diameter of the borehole:

$$SiO_2(\%) = 40.6 + (0.264\, I_o\, C) \qquad (3)$$

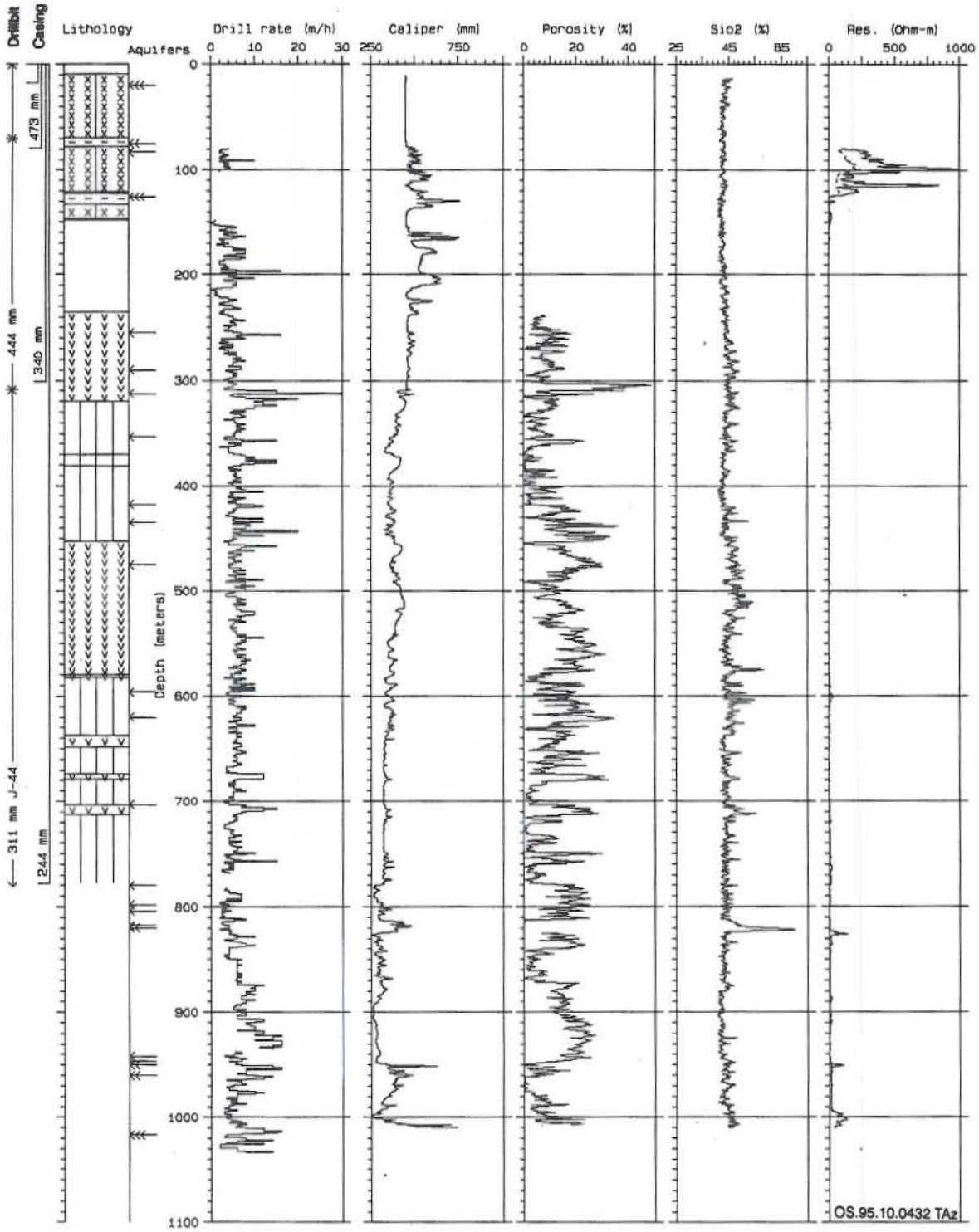

FIGURE 16: Porosity, SiO_2 and formation resistivity estimated from lithology logs in well ÖJ-1

$$C = \frac{1}{1.192 - 0.3937 \log[\frac{cal.(mm)}{20}]} - \frac{0.32}{[\frac{cal.(mm)}{20}]} \quad (4)$$

The BHMSIO2 programme was used to determine the SiO_2 content for well ÖJ-1. This programme is based on the above equations (Pordur Arason, 1995, pers. comm.). Figure 18 shows the estimated

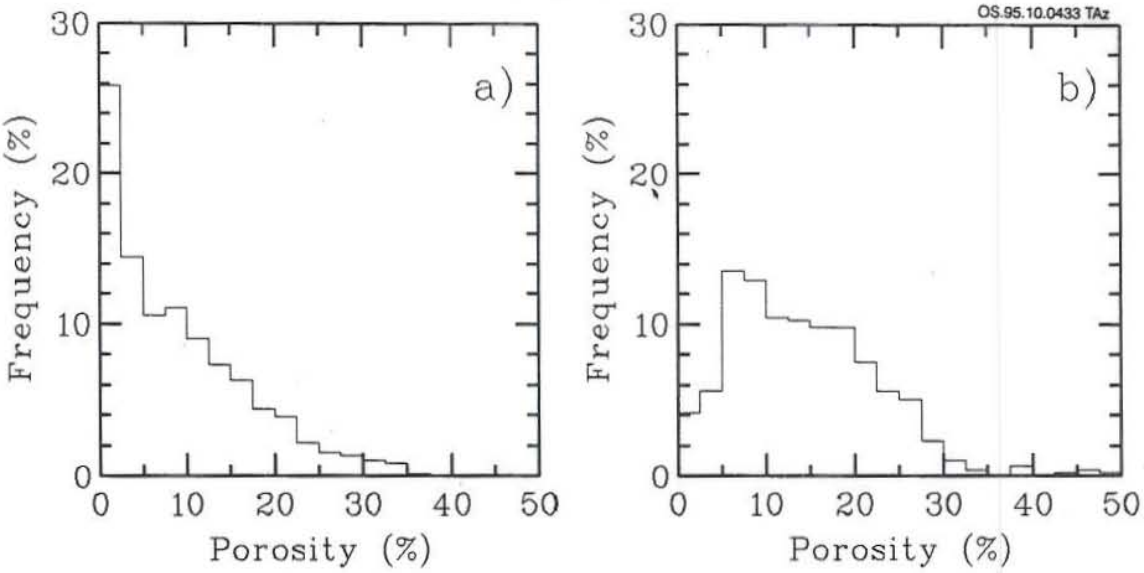

FIGURE 17: Distribution of estimated porosity for different rock types; a) basalt; b) tuff

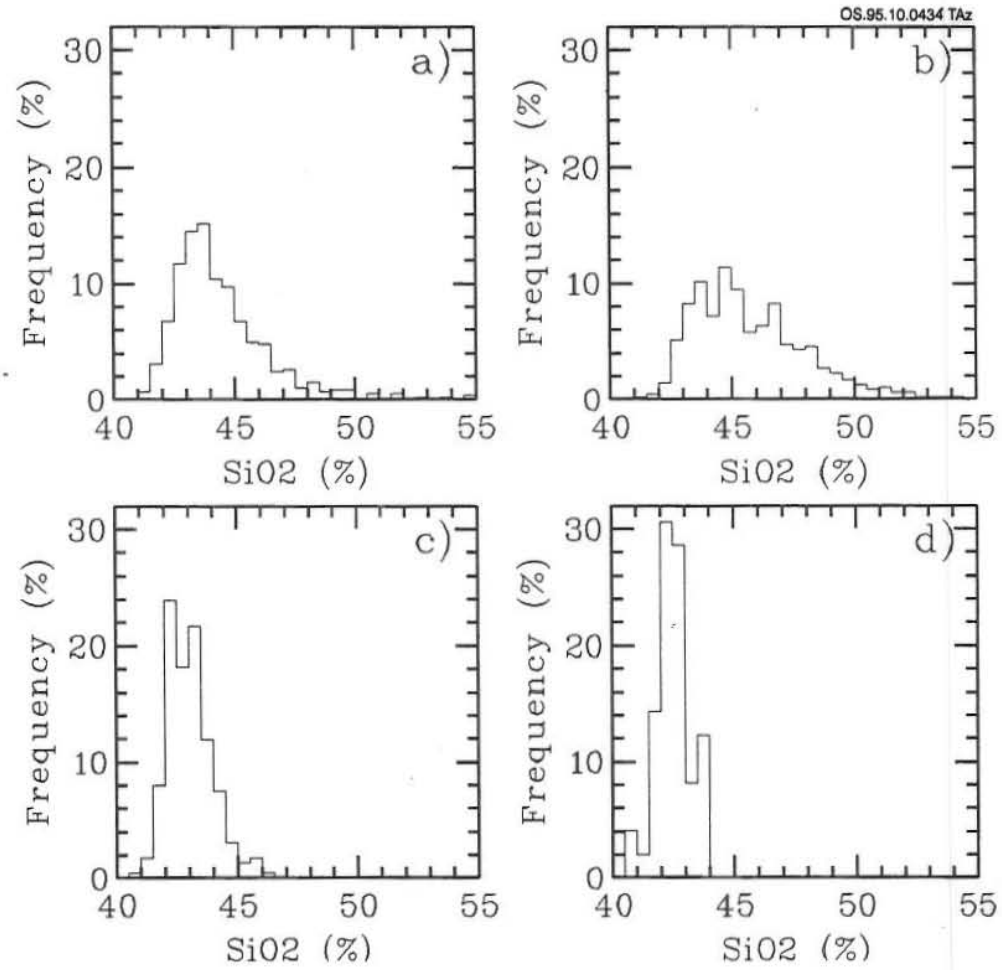

FIGURE 18: Distribution of estimated SiO_2 content for different rock types; a) altered basalt; b) altered tuff; c) fresh basalt and d) fresh tuff

distribution of SiO_2 for each of the four rock types: fresh basalt, altered basalt, fresh tuff and altered tuff. The fresh rock types have very sharp maxima between 42 and 45%, this represents the pure basaltic origin of the formation. The altered basalt or tuff is, however, different with the peak slightly higher (44% SiO_2) and the span wider. The standard deviation is also 2-3 times greater than that of the fresh rock. The difference may be due to secondary silica formed by deposition of geothermal minerals. This conclusion is also supported by the analysis of secondary minerals in the drill cuttings (Figure 19 and Hjalti Franzson 1995, pers. comm). However, these conclusions may not be correct, since the silica deposition may not follow the relationships presented in Equations 3 and 4.

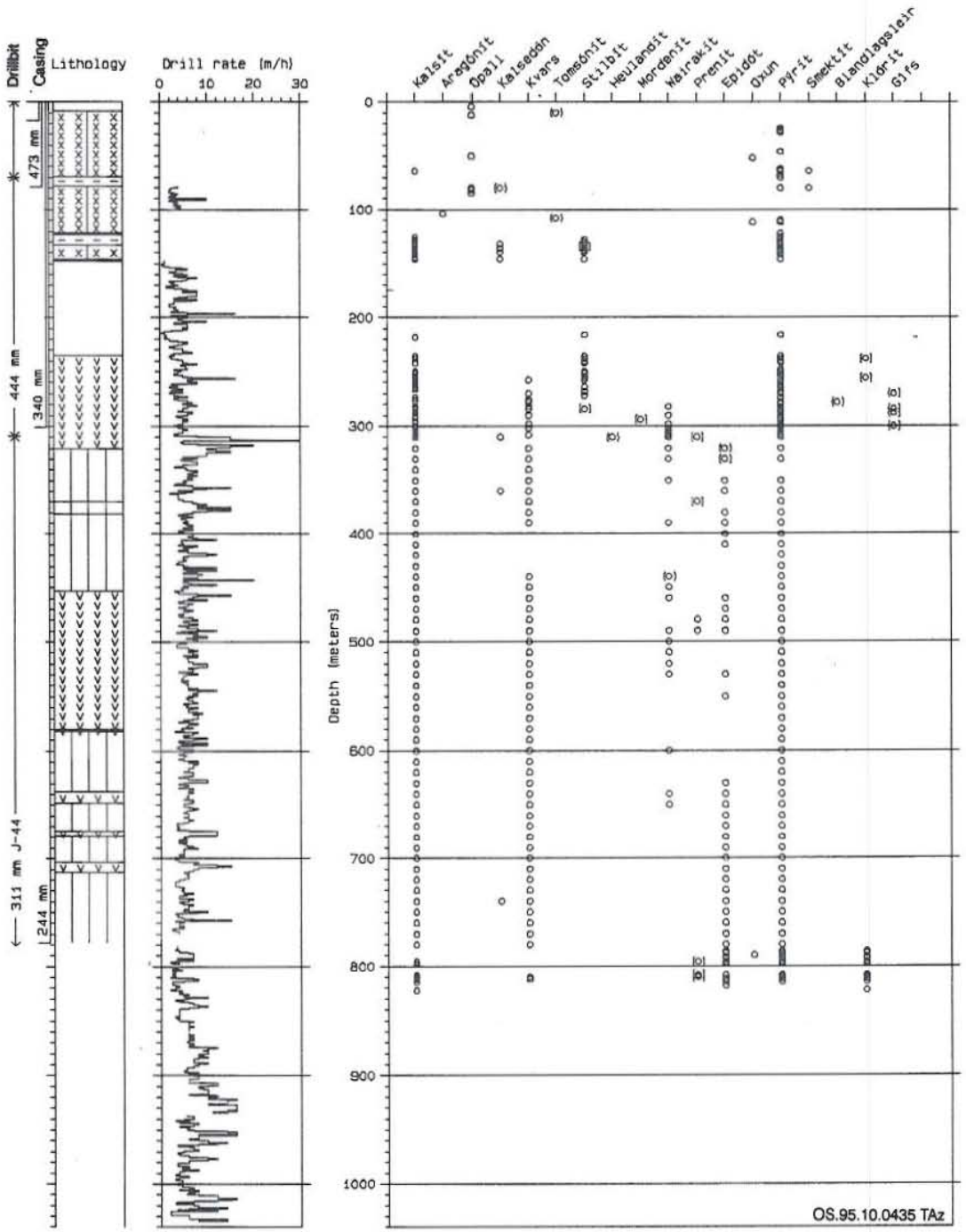

FIGURE 19: The occurrence of alteration minerals in the ÖJ-1 well

3.2.2 Well resistivity at undisturbed temperature conditions

Measurements of borehole resistivity in well ÖJ-1 were conducted at heavily disturbed conditions due to cooling of the formation and dilution of reservoir fluids caused by the drilling fluids. The measured resistivity does not only depend on the formation resistivity, but also on the width of the hole and the resistivity of the drilling fluids, which in turn depends on temperature as described by Equation 5. Therefore, some calculations must be done in order to evaluate the true formation resistivity. In this study, three computer programs were available to estimate the well resistivity at undisturbed formation conditions. They are based on the following equations (Björnsson et al., 1985):

$$\rho_w(T) = \frac{\rho_w(23\,°C)}{1 + 0.023\,(T - 23\,°C)} \tag{5}$$

$$\log \frac{\rho(T)}{\rho(30\,°C)} = Ax^2 + Bx + C \tag{6}$$

where

ρ_w = Fluid resistivity
ρ = Formation resistivity (Ωm)
x = $10^3/(T+273°C)$, $A = 0.475$, $B = -1.683$ and $C = 0.579$ are based on empirical formulae
T = Temperature during logging (°C).

The procedure is as follows. First, the resistivity is corrected for the influence of the drilling fluids, using the code RTW. In the case of well ÖJ-1, a 13 Ωm resistivity was assigned as fluid resistivity at 23°C (based on the average resistivity values of water samples from the Nesjavellir reservoir). At logging temperature it was corrected by using Equation 5. Secondly, RTC0 is a programme that calculates resistivity values at a constant 30°C temperature using Equation 6. Finally the RTC1 programme was used to calculate resistivity values at the estimated formation temperature by using Equation 6. Figure 16 shows this estimated formation resistivity profile of well ÖJ-1. The figure shows high resistivity (>80 Ωm) at shallow depth (0-120 m), but considerably lower resistivity (5-10 Ωm) beneath 120 m. A peak in the resistivity at 830 m is due to bleeding of gas into the wellbore during logging. However, high resistivity at around 1,000 m depth is most likely due to intrusive rock of higher density than the other formation layers.

3.3 Analysis of the core sample

A core sample was taken during the drilling of ÖJ-1 at 794.7-798.1 m depth. The total core recovery was 60%. From the core 11 plugs with a diameter of about 25 mm and lengths around 36 mm were sent for laboratory measurements, including measurements of porosity and resistivity. The analysis was conducted at room temperature and therefore, resistivity values must be calculated for formation temperature conditions (Sigurdsson, pers. comm.). Figure 20 shows how the core porosity and resistivity compare with the geophysical well logging data in Figure 16.

The core samples proved to be of about 13-19% porosity and about 10-35 Ωm resistivity. The analyses were done for the rock matrix, neglecting the influence of fractures. The lithological logs presented in Chapter 3.2 show porosity of the order of 15-20% and formation resistivity about 2 Ωm. Therefore there is good correlation of the porosity values between the lithological log calculation and the core analysis, taking into account that the calculated porosity reflects the total porosity of formation, whereas the

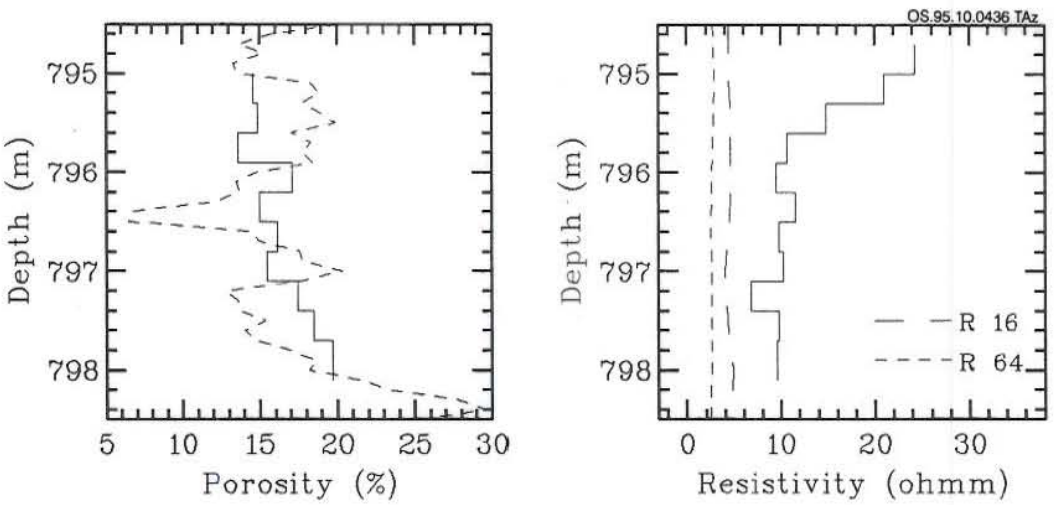

FIGURE 20: A comparison of core porosity and resistivity based on 11 samples (solid lines) with the calculated data from lithological logs (dashed lines)

measured porosity represents the effective porosity of the formation. The calculated resistivity values from the lithological logs are much lower than the core resistivity 5-20 Ωm. The reason for this is not well understood but may be due to fracturing in the formation.

4. SURFACE AND SUBSURFACE RESISTIVITY ANALYSIS

It is of interest to compare the resistivity observed directly in the well ÖJ-1 to the subsurface resistivity estimated by the TEM sounding measured at the surface (Chapter 2 and 3). Figure 21 shows this, i.e. the formation resistivity (Chapter 3) and the resistivity obtained by 1-D interpretation of the TEM station OH-16 (Chapter 2).

The figure shows a reasonable fit between these two independent data sources, in the upper part where both show drastic reduction in resistivity at 100 m depth. The resistivity in the depth interval 120-400 m is also similar, taking into account that the resistivity in the TEM sounding at 230-380 m is not well defined. However, at 400 m the TEM resistivity rises again in contrast to the downhole resistivity.

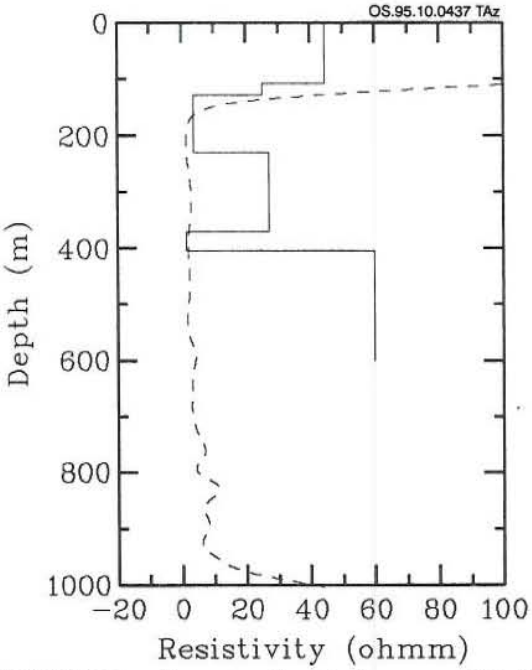

FIGURE 21: A comparison between resistivity measured directly in well ÖJ-1 (dashed line) and by TEM sounding OH16 (solid line)

5. WELL TESTING

Most high-temperature geothermal wells are tested at the end of drilling by injection tests. The purpose is to determine physical properties such as permeability and storativity of the reservoir penetrated by the well. An injection test was conducted in well ÖJ-1from January 21-22, 1995. During the test 9.9-27.3

l/s of water were pumped in steps into the well, each lasting 1-2 hours. Several temperature and pressure logs were carried out during the test.

5.1 Relative contribution of feedzones

Well ÖJ-1 has three major feedzones, at 820-827, 948-963, and 1000-1035 m. The bottom hole feedzone appears to be the dominant feedzone of the well and controlled the wellbore conditions at all times after intersection. These three feedzones appear to be in hydrostatic equilibrium when the temperature of the wellbore fluid equals the formation temperature. This equilibrium, however, goes out of balance when cold water is pumped into the well, leading to rapid internal flow in the well. Figure 22 demonstrates these phenomena clearly. The cold injection fluid travels down the well until 820-827 m, where the first feedzone is encountered. As the wellbore pressure at this depth is lower than the pressure in the reservoir, hot inflow takes place and causes a steplike temperature increase. A second inflow is encountered at the 948-963 m feedzone, leading to a further step increase in the wellbore temperature. This mixture of injected fluid and reservoir fluid is finally absorbed by the bottom hole feedzone, which controls the wellbore pressure due to its exceptionally high permeability.

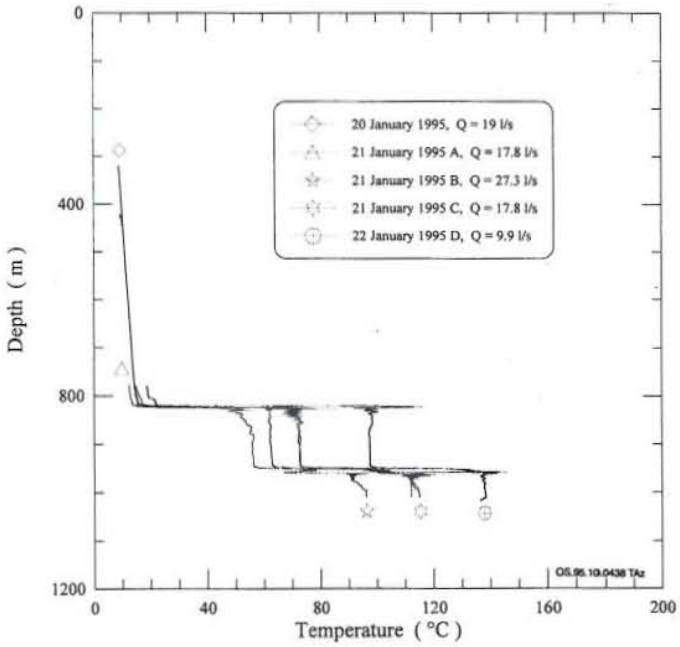

FIGURE 22: Temperature logs collected during the injection tests of well ÖJ-1

The temperature data in Figure 22 can be used to estimate the contribution of the two upper feedzones to the wellbore flow. According to Stefánsson and Steingrímsson (1980), the inflow q at a temperature T_l is given by the equation:

TABLE 1: Calculation of geothermal fluid entry into the feed zones of well ÖJ-1; the characters A, B, C and D refer to the downhole temperature profiles shown in Figure 22

Date of injections	Depth of feedzones (m)	Injection rate, Q (l/s)	Temperature T_o (°C)	Formation temperature, T_l (°C)	Total fluid entry, q (l/s)
A: 21.01.1995	823-825	17.8	19.0	197.9	7.6
	950-963			197.9	11.5
B: 21.01.1995	823-825	27.3	17.4	197.9	7.4
	950-961			197.9	13.7
C: 21.01.1995	820-827	17.8	18.5	197.9	9.6
	950-961			197.9	11.1
D: 22.01.1995	820-823	9.9	19.1	197.9	7.4
	950-958			197.9	11.8

$$q = Q_o \frac{T - T_o}{T_1 - T} \tag{7}$$

where Q_o and T_o present the flow and temperature above the inflow aquifer respectively, and T is the temperature below the aquifer. The above equation applies to single phase fluids only. Table 1 shows the inflow rates at each of the feedzones and the different injection rates. It should be noted that the formation temperature was used as the temperature of the two feedzones.

As mentioned before, the 9.9-27.3 l/s of 11°C water were injected continuously when pressure and temperature loggings were carried out. To the injection rate, approximately 20 l/s (see Table 1) must be added in order to explain the flow into the bottom feedzone. Figure 23 shows the injection rate, total flow and pressure at 780 m depth with time during the injection test.

Figures 23 and 24 show a very unusual pressure response to injection, which are, the pressure drops as the injection rate is increased and the pressure increases when the injection rate is lowered. This extraordinary pressure response is caused by temperature variations in the well (density variations) which makes traditional well test analysis impossible. Therefore, it can only be concluded that the reservoir permeability close to well ÖJ-1 is very high. This trend of declining pressure with increased injection rates is known in vapour-dominated reservoirs where the effect of steam condensation or temperature variations caused by internal flow in the well may cause it. The reservoir temperature in well ÖJ-1 is, however, well below saturation and does not allow any boiling or condensation at this depth of the well. It is therefore suggested that the feedzones of well ÖJ-1 are associated with a near vertical fracture

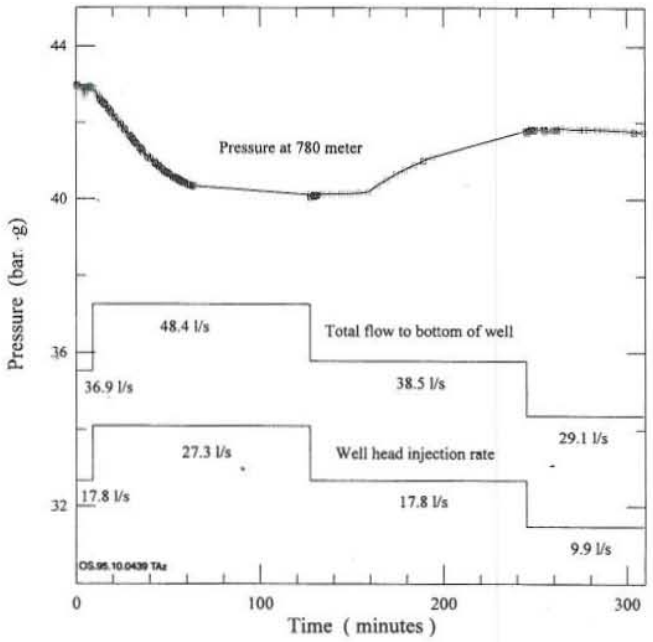

FIGURE 23: Wellhead injection rate, total flow to bottom of well and pressure at 780 m depth during the injection test in well ÖJ-1

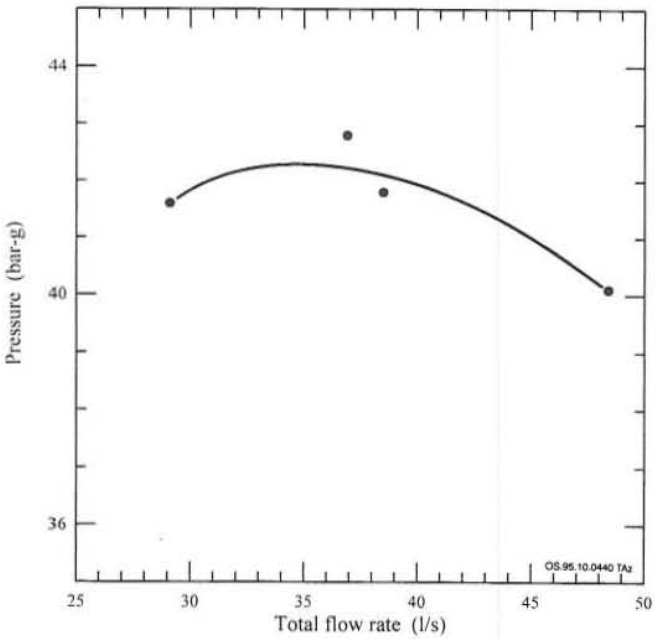

FIGURE 24: Total flow rate into the bottomhole feedzone vs. pressure at 780 m depth in well ÖJ-1

of high permeability. As the cold injection fluid enters this fracture, the high fluid density leads to downflow and pressure stabilization in a reservoir volume at great depths. Therefore, productivity of the well does not depend on the capability of the formation to supply geothermal fluids but on the production design of the well itself. In other words the productivity is controlled by the well diameter.

5.2 Flowing pressure and temperature survey

Well ÖJ-1 flowed for a few weeks during the autumn of 1995. The downhole pressures and temperatures were measured during the flow test. It is of interest to simulate the downhole data and analyse in terms of wellhead output curves.

The wellbore simulator HOLA was used for this purpose (Björnsson et al., 1993). It solves numerically the differential equations that describe the steady-state energy, mass and momentum flow in a vertical pipe. The governing equations are given as follows:

$$\frac{dm}{dz} = 0 \tag{8}$$

$$\frac{dP}{dz} - [(\frac{dP}{dz})_{fri} + (\frac{dP}{dz})_{acc} + (\frac{dP}{dz})_{pot}] = 0 \tag{9}$$

$$\frac{dE_t}{dz} \pm Q = 0 \tag{10}$$

where

m	= Total mass flow in the well (kg/s)
z	= Depth coordinates (m)
P	= Pressure (Pa)
E_t	= Total energy flux in the well (J/s)
Q	= Ambient heat losses over a unit distance (W/m)
$(dP/df)_{fri}$	= Pressure gradient due to wall friction (Pa/m)
$(dP/dz)_{acc}$	= Pressure gradient due to acceleration of the fluid (Pa/m)
$(dP/dz)_{pot}$	= Change in gravitational load over dz (Pa/m)
+/-	= Upward/downward flow, respectively.

The governing equation of flow between the well and the reservoir can be estimated as

$$m_{feed} = PI \frac{k_r \rho}{\mu}(P_r - P_w) \tag{11}$$

where

m_{feed}	= feedzone flowrate (kg/s)
PI	= productivity index of the feedzone (m^3/s bar)
k_r	= relative permeability of the phase (subscripts *l* for liquid and *g* for steam)
μ	= dynamic viscosity (kg/ms)
ρ	= density (kg/m^3)
P_r	= reservoir pressure (Pa)
P_w	= pressure in the well (Pa)

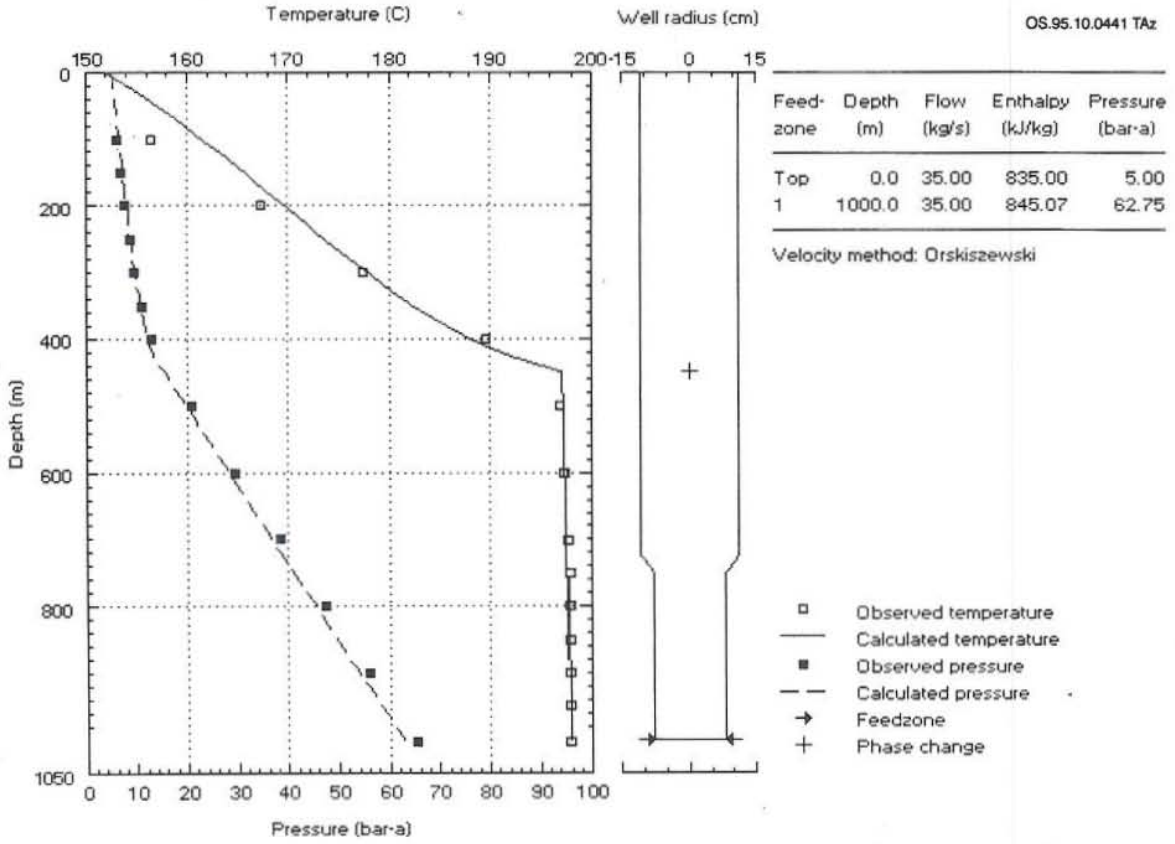

FIGURE 25: Measured and calculated downhole temperature and pressure profiles in well ÖJ-1 based on the programme HOLA

As mentioned before, the last measurements of temperature and pressure logs were conducted during flowing conditions, where flowrate and discharge enthalpy were observed to be about 33 kg/s and 830 kJ/kg. The HOLA wellbore simulator was used to calculate wellhead conditions. Figure 25 shows a good match between the observed and the calculated, temperature and pressure values at flowrate of about 35 kg/s and discharge enthalpy 835 kJ/kg when the velocity method of Orskiszewski was used.

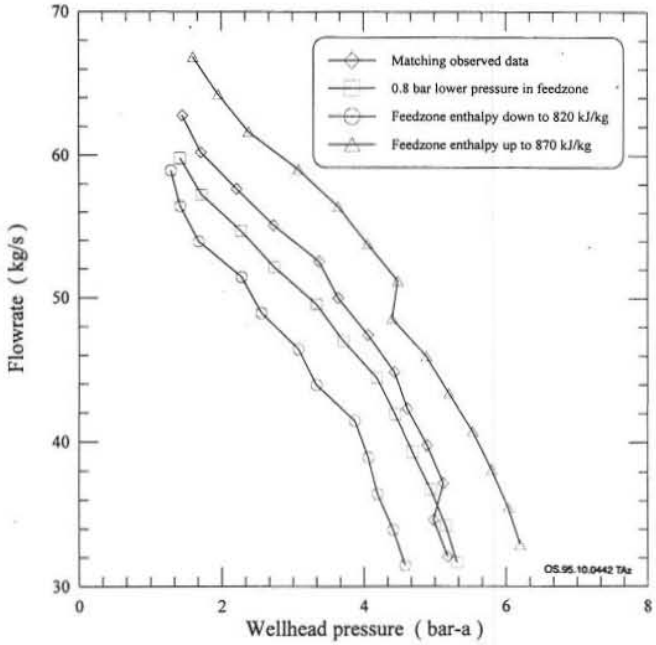

FIGURE 26: A simulation of productivity by changing pressure and enthalpy of feedzones in well ÖJ-1

The HOLA wellbore simulator can also be used to estimate the wellhead output curves for well ÖJ-1. By assigning a one bar-a wellhead pressure, assuming an initial flowing bottomhole pressure of 62.1 bar-a and a feedzone pressure of 62.8 bar-a, a trial and error procedure gave a 0.8×10^{-11} m^3 productivity index for the well. Figure 26 shows the relation between wellhead flowrate and wellhead pressure for this productivity index and also additional output curves where the reservoir pressure and enthalpy have been varied. The figure shows that for reducing reservoir pressure and enthalpy, the output curve will shift to the left-hand side. It means reduction of the capability of the well to supply geothermal fluids.

6. SUMMARY AND CONCLUSIONS

The Ölkelduháls geothermal field is a part of the Hengill high-temperature geothermal area in SW-Iceland, about 30 km from Reykjavík. Exploration of the field includes a conduction of several resistivity surveys applying Schlumberger soundings and recently also TEM soundings in order to define the distribution of resistivity in the area and correlate it to the geothermal activity. During the winter 1994-1995 the first exploration well, ÖJ-1, was drilled at Ölkelduháls. Interpretation of TEM soundings, analysis of logging data and comparison between the two was the scope of the study presented in this report. The main results of the study can be summarized as follows:

1. The geothermal activity of the Ölkelduháls field is associated with a resistivity low at a shallow depth (<5 Ωm at 100-300 m depth). Below this, a high resistivity core is found.

2. The resistivity anomaly covers an area of 20 km^2 or about one fifth of the whole Hengill geothermal area.

3. The change with depth from low to high resistivity in Ölkelduháls coincides with the change in alteration observed in well ÖJ-1 (according to drill cuttings analysis) where clay minerals disappear and high-temperature minerals such as wairakites and epidotes become common.

4. TEM soundings and Schlumberger measurements provide similar resistivity distributions with depth. TEM data give, however, a better depth resolution and accuracy.

5. Well ÖJ-1 shows the existence of cold/warm aquifers above 120 m depth with water levels at 14-33 m depth. From 120 to about 400 m depth the formation temperature increases from 20 to 200°C, where the top of an isothermal geothermal reservoir is reached. This 200°C reservoir extends beyond the bottom of the well at 1035 m depth. The geothermal reservoir has much lower pressure potential than the shallow cold/warm aquifers.

6. A comparison of the resistivity distribution, determined by TEM soundings close to the well ÖJ-1 and well data, shows good correlation at shallow depth. High resistivity is found above 120 m both in the well resistivity logs and TEM soundings. Below the 120 m the observed formation resistivity in the well is of the order of a few Ωm all the way to 1000 m depth, in some agreement with low resistivity in the TEM soundings down to 300 m depth where the high-resistivity layer is encountered. The absence of this high-resistivity in the well logs has not been explained and must wait for further studies.

7. A comparison of well logging data and laboratory measurements, done on a three metre long core sample, revealed good correlation between porosity values. The resistivity values were, however, quite different, with logging values of the order of 3-5 Ωm but 10-25 Ωm for the core.

8. The major feedzones of well ÖJ-1 are at 820-827, 948-963 and 1000-1035 m depth. All the feedzones are highly permeable and during injection tests internal flow dominated the pressure response of the well. About 20 l/s flowed into the well through the uppermost two feedzones and joined the injected water in it, which flows towards the bottom feedzone, the best feedzone of the well.

9. Analysis of flowing temperature and pressure surveys using the wellbore simulator HOLA, confirms the extremely high permeability of the well and gives a productivity index of 0.8×10^{-11} m^3/s bar. This means that the well configuration (diameter) controls the flow from the well.

ACKNOWLEDGMENTS

I want to thank all involved for giving me an opportunity to participate in the UNU Geothermal Training Programme, especially Dr. Ingvar Birgir Fridleifsson, director of the Programme and the management of PERTAMINA for the permission to attend this specialized course. Thanks to Mr. Grímur Björnsson, Mr. Benedikt Steingrímsson and Ms. Helga Tulinius, my advisers, for sharing their knowledge and experience, also for great help and critical advice to expand this report. Also, thanks to all the staff at Orkustofnun for their willingness to help.

Special thanks go to Mr. Lúdvík S. Georgsson (also my advisor) for all the help and care during the whole training period. And thanks to Ms. Súsanna Westlund and Ms. Margrét Westlund for their wonderful care.

REFERENCES

Arason, P., 1993: *The BHM programme*. Orkustofnun, Reykjavík, Iceland.

Árnason, K., 1989: *Central loop transient electromagnetic soundings over a horizontally layered earth.* Orkustofnun, Reykjavík, report OS-89032/JHD-09, 128 pp.

Árnason, K., 1993: *Geothermal activity in the Ölkelduháls area, resistivity soundings in 1991 and 1992.* Orkustofnun, Reykjavík, report OS-93037/JHD-10 (in Icelandic), 82 pp.

Árnason, K., and Flóvenz Ó.G., 1992: Evaluation of physical methods in geothermal exploration of rifted volcanic crust. *Geoth. Res. Council, Transactions, 16,* 207-214.

Björnsson, A., Hersir, G.P., and Björnsson, G., 1986: The Hengill high-temperature area SW-Iceland: Regional geophysical survey. *Geoth. Res. Council, Transactions, 10,* 205-210.

Björnsson, A., Saemundsson, K., Árnason, K., Björnsson, G., Hersir, G.P., and Johnsen, G.V., 1985: *Nesjavellir - Geothermal exploration.* Orkustofnun, Reykjavík, report OS-85030/JHD-07 (in Icelandic), 97 pp.

Björnsson, G., 1993: Programme PREDYP. In: Árnason, P., and Björnsson, G. (collected in 1994), *ICEBOX, 2nd edition, user's guide.* Orkustofnun, Reykjavík.

Björnsson, G., Arason, P., and Bödvarsson, G., 1993: *The wellbore simulator HOLA, version 3.1, user's guide.* Orkustofnun, Reykjavík.

Georgsson, L.S., Árnason, K., and Karlsdóttir, R., 1993: Resistivity sounding in high-temperature areas in Iceland, with examples from Öxarfjördur, N-Iceland and Brennisteinsfjöll, SW-Iceland. *14th PNOC-EDC Geothermal Conference, Manila, Philippines,* 9 pp.

Gudmundsson, Á., Steingrímsson, B., Sigursteinsson, D., Björnsson, G., Sigvaldason, H., Franzson, H., Hólmjárn, J., Sigurdsson, Ó., Benediktsson, S., and Thórhallsson, S., 1994: *The Ölkelduháls field, well ÖJ-1, 1st drilling phase.* Orkustofnun, Reykjavík, report OS-94056/JHD-33 B (in Icelandic), 20 pp.

Gudmundsson, Á., Steingrímsson, B., Sigursteinsson, D., Björnsson, G., Sigvaldason, H., Franzson, H., Hólmjárn, J., Sigurdsson, Ó., Benediktsson, S., and Thórhallsson, S., 1995a: *The Ölkelduháls field, well ÖJ-1, 2nd drilling phase.* Orkustofnun, Reykjavík, report OS-95001/JHD-01 B (in Icelandic), 28 pp.

Gudmundsson, Á., Steingrímsson, B., Sigursteinsson, D., Björnsson, G., Sigvaldason, H., Franzson, H., Hólmjárn, J., Sigurdsson, Ó., Benediktsson, S., and Thórhallsson, S., 1995b: *The Ölkelduháls field, well ÖJ-1, 3rd drilling phase.* Orkustofnun, Reykjavík, report OS-95007/JHD-05 B (in Icelandic), 25 pp.

Gunnarsson, Á., Steingrímsson, B.S., Gunnlaugsson, E., Magnússon, J., and Maack, R., 1992: Nesjavellir geothermal co-generation power plant. *Geothermics, 21-4,* 559-583.

Hersir, G.P., and Björnsson, A., 1991: *Geophysical exploration for geothermal resources, principles and application.* UNU G.T.P., Iceland, report 15, 94 pp.

Keys, W.S., and McCary, L.M., 1971: Application of borehole geophysics to water-resources investigation. In: *Techniques of Water-Resources Investigations.* Geological Survey, Book 2, Sec. E, Washington., USA, 126 pp.

Saemundsson, K., 1979: Outline of the geology of Iceland, *Jökull, 29,* 7-28.

Saemundsson, K., Snorrason, S.P., and Fridleifsson, G.Ó., 1990: *Geological map of the southern Hengill area, between Hengladalir and Krossfjöll.* Orkustofnun, Reykjavík, report OS-90008/JHD-02 B, 15 pp.

Stefánsson, V., Gudmundsson, Á., and Emmerman, R., 1982: Gamma ray activity in Icelandic rocks. *The Log Analyst, XXIII-6,* 11-16.

Stefánsson, V., and Steingrímsson, B., 1980: *Geothermal logging I, an introduction to techniques and interpretation.* Orkustofnun, Reykjavík, report OS-80017/JHD-09, 117 pp.

APPENDIX I: TEM soundings in the Ölkelduháls area

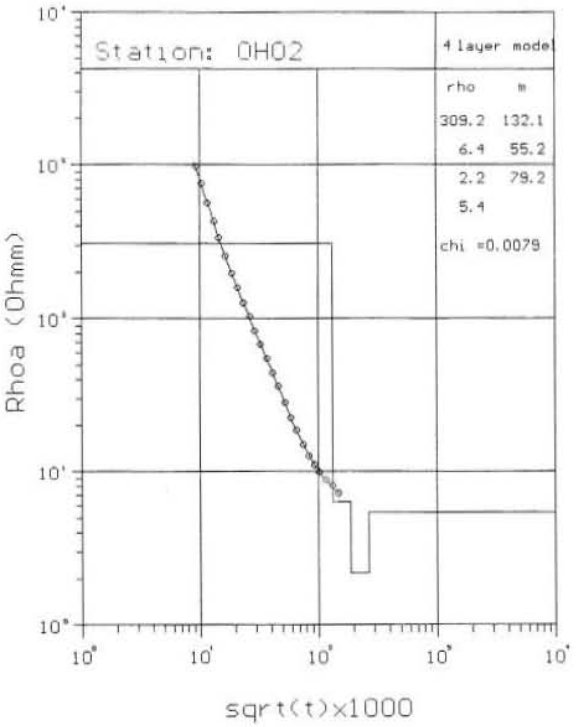

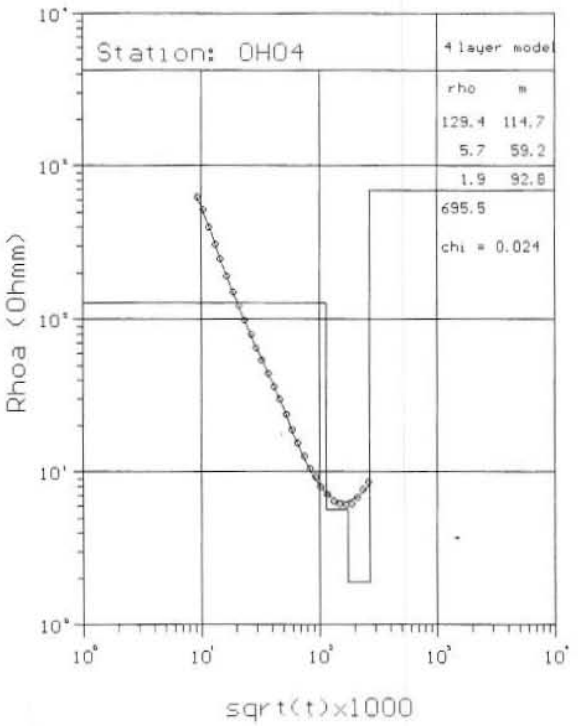

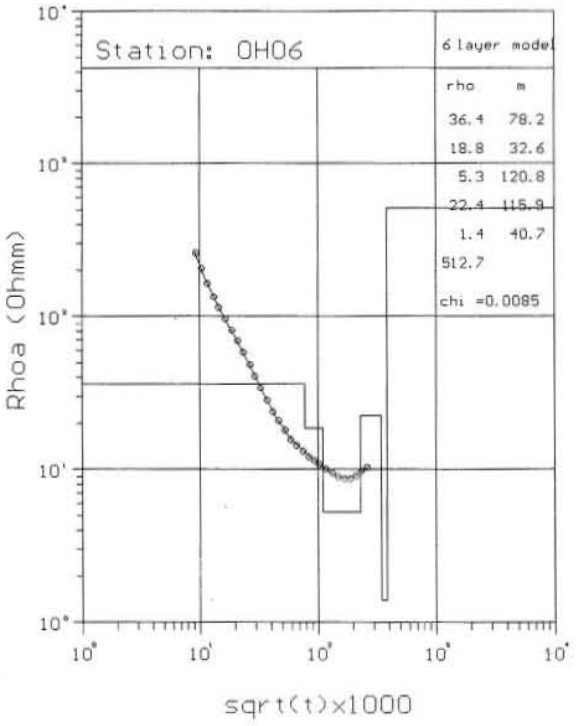

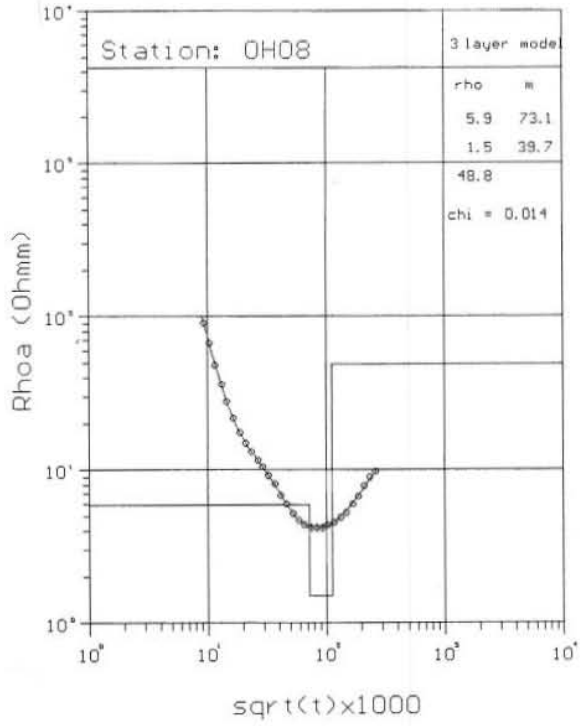

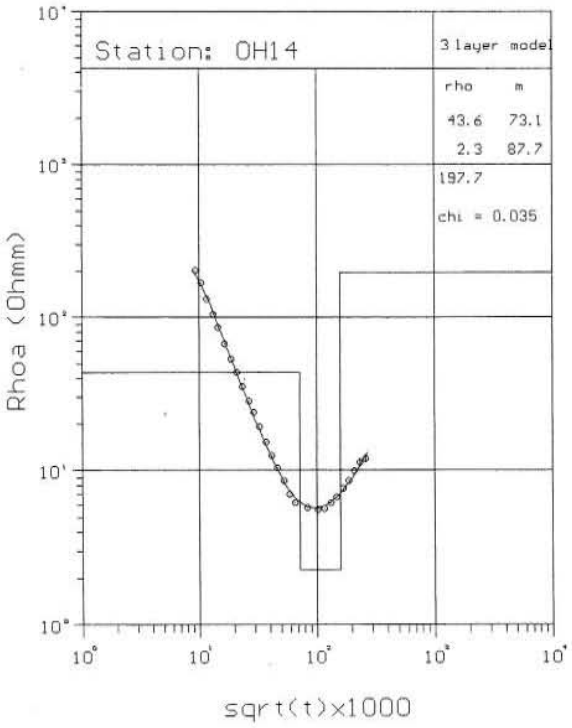
Station: OH14
3 layer model
rho m
43.6 73.1
2.3 87.7
197.7
chi = 0.035
Rhoa (Ohmm)
sqrt(t)x1000

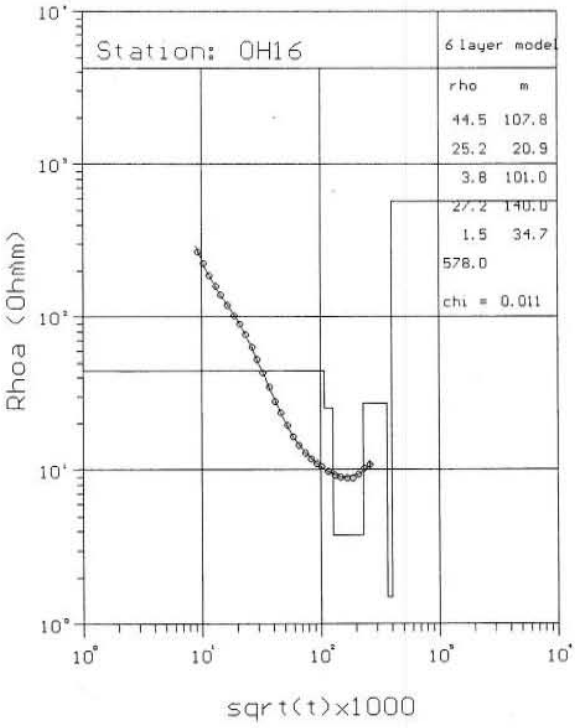
Station: OH16
6 layer model
rho m
44.5 107.8
25.2 20.9
3.8 101.0
27.2 140.0
1.5 34.7
578.0
chi = 0.011
Rhoa (Ohmm)
sqrt(t)x1000

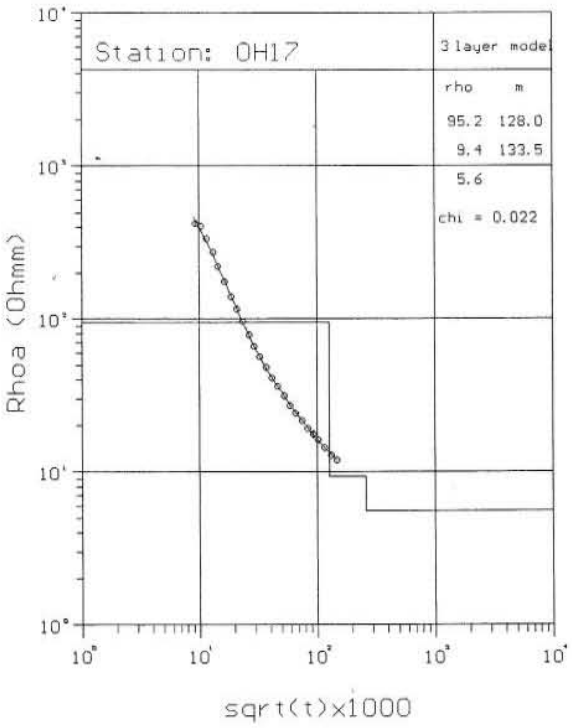
Station: OH17
3 layer model
rho m
95.2 128.0
9.4 133.5
5.6
chi = 0.022
Rhoa (Ohmm)
sqrt(t)x1000

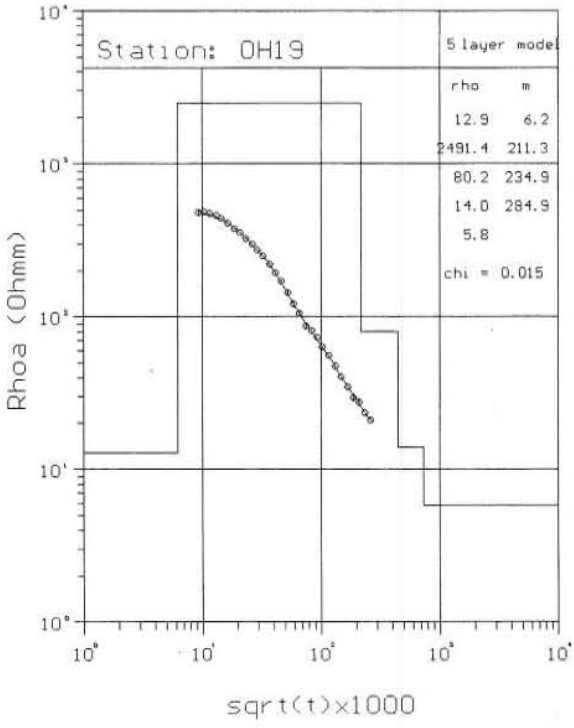
Station: OH19
5 layer model
rho m
12.9 6.2
2491.4 211.3
80.2 234.9
14.0 284.9
5.8
chi = 0.015
Rhoa (Ohmm)
sqrt(t)x1000

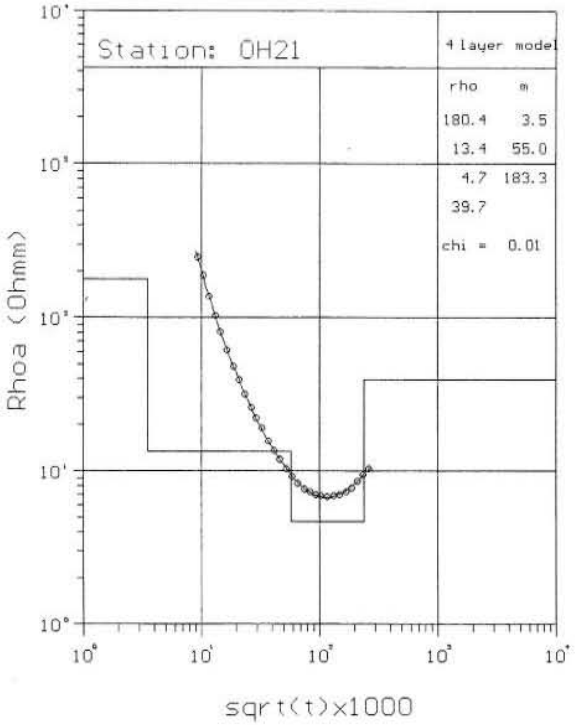
Station: 0H21
4 layer model
rho m
180.4 3.5
13.4 55.0
4.7 183.3
39.7
chi = 0.01
Rhoa (Ohmm)
sqrt(t)x1000

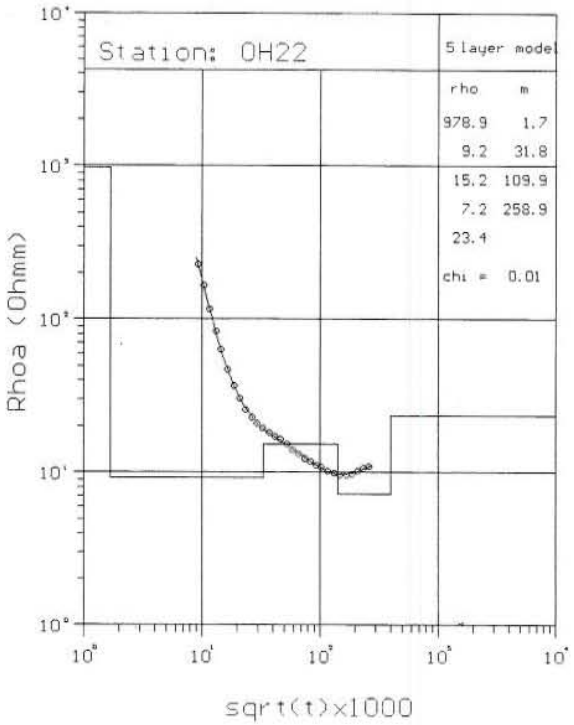
Station: 0H22
5 layer model
rho m
978.9 1.7
9.2 31.8
15.2 109.9
7.2 258.9
23.4
chi = 0.01
Rhoa (Ohmm)
sqrt(t)x1000

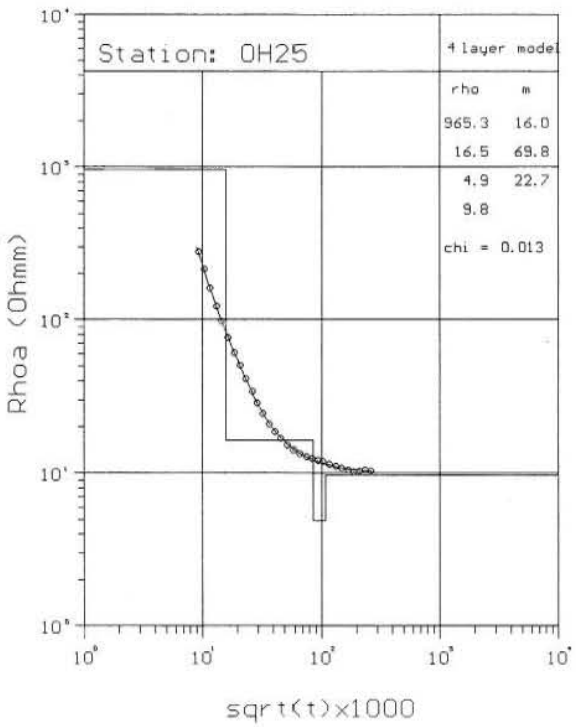
Station: 0H25
4 layer model
rho m
965.3 16.0
16.5 69.8
4.9 22.7
9.8
chi = 0.013
Rhoa (Ohmm)
sqrt(t)x1000